









# The lysosomal Ragulator complex activates NLRP3 inflammasome *in vivo* via HDAC6

Kohei Tsujimoto<sup>1,2,3,†</sup> , Tatsunori Jo<sup>1,2,†</sup> , Daiki Nagira<sup>1,2,3</sup>, Hachiro Konaka<sup>1,2,3</sup>, Jeong Hoon Park<sup>4</sup>, Shin-ichiro Yoshimura<sup>5</sup> , Akinori Ninomiya<sup>6</sup> , Fuminori Sugihara<sup>6</sup>, Takehiro Hirayama<sup>1,2,3</sup>, Eri Itotagawa<sup>1,2,3</sup>, Yusei Matsuzaki<sup>3,7</sup>, Yuki Takaichi<sup>3,7</sup>, Wataru Aoki<sup>3,7</sup>, Shotaro Saita<sup>8</sup>, Shuheï Nakamura<sup>8,9</sup> , Andrea Ballabio<sup>10,11,12,13,14</sup> , Shigeyuki Nada<sup>15</sup>, Masato Okada<sup>15</sup>, Hyota Takamatsu<sup>1,2,3,\*</sup>  & Atsushi Kumanogoh<sup>1,2,3,16,17,18,\*\*</sup> 

## Abstract

The cellular activation of the NLRP3 inflammasome is spatiotemporally orchestrated by various organelles, but whether lysosomes contribute to this process remains unclear. Here, we show the vital role of the lysosomal membrane-tethered Ragulator complex in NLRP3 inflammasome activation. Deficiency of Lamtor1, an essential component of the Ragulator complex, abrogated NLRP3 inflammasome activation in murine macrophages and human monocytic cells. Myeloid-specific Lamtor1-deficient mice showed marked attenuation of NLRP3-associated inflammatory disease severity, including LPS-induced sepsis, alum-induced peritonitis, and monosodium urate (MSU)-induced arthritis. Mechanistically, Lamtor1 interacted with both NLRP3 and histone deacetylase 6 (HDAC6). HDAC6 enhances the interaction between Lamtor1 and NLRP3, resulting in NLRP3 inflammasome activation. DL-all-rac- $\alpha$ -tocopherol, a synthetic form of vitamin E, inhibited the Lamtor1–HDAC6 interaction, resulting in diminished NLRP3 inflammasome activation. Further, DL-all-rac- $\alpha$ -tocopherol alleviated acute gouty arthritis and MSU-induced peritonitis. These results provide novel insights into the role of lysosomes in the activation of NLRP3 inflammasomes by the Ragulator complex.

**Keywords** HDAC6; NLRP3 inflammasome; Ragulator complex;  $\alpha$ -tocopherol

**Subject Categories** Immunology; Organelles

**DOI** 10.15252/embj.2022111389 | Received 7 April 2022 | Revised 26 October 2022 | Accepted 2 November 2022 | Published online 29 November 2022

**The EMBO Journal (2023) 42: e111389**

## Introduction

Lysosomes are dynamic organelles that can change their morphology, localization, and quantity in response to various stimuli, and in this manner, contribute to the degradation of extracellular and intracellular waste products (Ballabio & Bonifacino, 2020). In addition to their degradative roles, recent studies have shown that lysosomes are involved in a variety of tasks related to nutrient sensing, immune cell signaling, metabolism, and membrane repair (Perera & Zoncu, 2016; Jia *et al.*, 2018; Condon *et al.*, 2021). Lysosomes serve as a signaling hub to integrate extracellular and intracellular stimuli and thus regulate cellular homeostasis. Furthermore, lysosomes are closely involved in the regulation of inflammation, and abnormalities in lysosomal function result in a broad range of diseases (Perera & Zoncu, 2016; Ballabio & Bonifacino, 2020).

- 1 Department of Respiratory Medicine and Clinical Immunology, Graduate School of Medicine, Osaka University, Osaka, Japan
  - 2 Department of Immunopathology, Immunology Frontier Research Center (iFReC), Osaka University, Osaka, Japan
  - 3 The Japan Science and Technology – Core Research for Evolutional Science and Technology (JST–CREST), Osaka University, Osaka, Japan
  - 4 Department of Internal Medicine, Daini Osaka Police Hospital, Osaka, Japan
  - 5 Department of Cell Biology, Graduate School of Medicine, Osaka University, Osaka, Japan
  - 6 Central Instrumentation Laboratory, Research Institute for Microbial Diseases, Osaka University, Osaka, Japan
  - 7 Division of Applied Life Sciences, Graduate School of Agriculture, Kyoto University, Kyoto, Japan
  - 8 Department of Genetics, Graduate School of Medicine, Osaka University, Osaka, Japan
  - 9 Institute for Advanced Co-Creation Studies, Osaka University, Osaka, Japan
  - 10 Telethon Institute of Genetics and Medicine (TIGEM), Pozzuoli, Italy
  - 11 Medical Genetics Unit, Department of Medical and Translational Science, Federico II University, Naples, Italy
  - 12 Department of Molecular and Human Genetics, Baylor College of Medicine, Houston, TX, USA
  - 13 Jan and Dan Duncan Neurological Research Institute, Texas Children's Hospital, Houston, TX, USA
  - 14 Scuola Superiore Meridionale (SSM), School for Advanced Studies, Federico II University, Naples, Italy
  - 15 Department of Oncogene Research, Research Institute for Microbial Diseases, Osaka University, Osaka, Japan
  - 16 Integrated Frontier Research for Medical Science Division, Institute for Open and Transdisciplinary Research Initiatives (OTIR), Osaka University, Osaka, Japan
  - 17 Center for Advanced Modalities and DDS (CAMaD), Osaka University, Osaka, Japan
  - 18 Center for Infectious Diseases for Education and Research (CIDER), Osaka University, Suita, Japan
- \*Corresponding author. Tel: +81 6 6879 3833; E-mail: Hyota Takamatsu, E-mail: thyota@imed3.med.osaka-u.ac.jp  
 \*\*Corresponding author. Tel: +81 6 6879 3831; E-mail: Atsushi Kumanogoh, E-mail: kumanogo@imed3.med.osaka-u.ac.jp  
 †These authors contributed equally to this work

The Ragulator complex, a lysosomal membrane protein, is a pentamer containing Lamtor1/p18, Lamtor2/p14–Lamtor3/MP1, and Lamtor4/p10–Lamtor5/HBXIP (Yonehara *et al*, 2017). Lamtor1 wraps around Lamtor2–5 stabilizing the Ragulator complex and the protein levels of Lamtor2–5 are reduced in cases of Lamtor1 deficiency (Nakatani *et al*, 2021). The mechanistic target of rapamycin (mTOR), a master regulator of cellular metabolism, is present in two distinct complexes, mTORC1 and mTORC2 (Liu & Sabatini, 2020). mTOR functions as a serine/threonine kinase regulating diverse cellular homeostasis like cell proliferation, cell death, protein synthesis, and autophagy by participating in multiple signaling pathways (Saxton & Sabatini, 2017; Liu & Sabatini, 2020). The localization of mTORC1 is important for the regulation of activity and it is activated on lysosomes in response to nutrients. The Ragulator complex plays a critical role in the mTOR signal transduction pathway by tethering the mTORC1 complex to the lysosomal surface (Kim *et al*, 2008; Sancak *et al*, 2010; Yonehara *et al*, 2017). Lamtor1 is directly responsible for anchoring the Ragulator complex to the lysosomal membrane, where it then tethers the Rag GTPase heterodimers RagA/B and RagC/D (de Araujo *et al*, 2017; Yonehara *et al*, 2017). The pleiotropic roles of the Ragulator complex can regulate many cellular functions other than those of mTORC1 by interacting with various proteins. The Ragulator complex is a platform for maintaining cellular homeostasis such as integrin signaling via Lamtor2–MEK, acidification of lysosomes via V-type ATPase, lysosome biogenesis by enhanced TFEB nuclear translocation, endomembrane damage repair or organelle homeostasis, and the regulation of migration through interactions with the myosin phosphatase–Rho interacting protein (MPRIIP; Nada *et al*, 2009; Yonehara *et al*, 2017; Jia *et al*, 2018; Ballabio & Bonifacino, 2020; Condon *et al*, 2021; Nakatani *et al*, 2021). Several other studies have supported the role of the Ragulator complex as an inflammatory platform, i.e., for M2 differentiation and TFEB-mediated cytokine production (Kimura *et al*, 2016; Hayama *et al*, 2018). In addition, the role of the Ragulator complex in the regulation of cell death has received a great deal of attention (Zheng *et al*, 2021; preprint: Colville *et al*, 2022; Hein & Weissman, 2022). In particular, in recent years there has been a series of important reports regarding the relationship between the Ragulator complex and pyroptosis, a type of inflammatogenic caspase-1-dependent cell death (Evavold *et al*, 2021; preprint: Devant *et al*, 2022). In pyroptosis, the Ragulator complex plays an essential role in the regulation of gasdermin D (GSDMD) oligomerization and pore formation.

GSDMD is a key regulator of pyroptosis and the secretion of inflammatory cytokines such as IL-1 $\beta$  and is itself regulated by inflammasome activation (Evavold & Kagan, 2019). NLR family pyrin domain-containing 3 (NLRP3) is one of the most well-characterized inflammasomes, and it reacts to a wide range of inflammatory infectious and endogenous ligands, such as pathogen-associated molecular patterns (PAMPs) and damage-associated molecular patterns (DAMPs; Swanson *et al*, 2019). After exposure to PAMPs or DAMPs, NLRP3 binds to apoptosis-associated speck-like protein containing a CARD (ASC) to form the inflammasome complex, resulting in the cleavage of inactive pro-caspase-1 to produce active caspase-1 and subsequent cleavage of proinflammatory cytokines and GSDMD (Franchi *et al*, 2009). NLRP3 inflammasome activation and subsequent IL-1 $\beta$  secretion occur via a three-step process (Evavold & Kagan, 2019). The first or priming step is the

activation of the nuclear factor kappa B (NF- $\kappa$ B) pathway, leading to the upregulation of NLRP3 and pro-IL-1 $\beta$  proteins and to changes in post-translational modifications such as the phosphorylation or ubiquitination of NLRP3 and ASC. The second or activation step leads to active inflammasome complex formation and consequently, the production of the active form of Caspase-1 and GSDMD. The third step is the release of the mature form of IL-1 $\beta$  out of the cells through the GSDMD pores. Recently, the involvement of the Ragulator complex in GSDMD regulation has been reported (Evavold *et al*, 2021; preprint: Devant *et al*, 2022). Devant and colleagues (preprint: Devant *et al*, 2022) also reported that the Ragulator complex is required for reactive oxygen species (ROS) production, which enables the oligomerization and pore formation of GSDMD. However, the precise role of the Ragulator complex in NLRP3 inflammasome activation, especially in the activation phase, requires elucidation.

The activation of NLRP3 inflammasomes is tightly regulated by numerous processes that are coordinated by its spatiotemporal dynamics. Upon stimulation, NLRP3 dynamically moves from the cytosol to the mitochondria-associated membrane (MAM) and finally to the microtubule-organizing center (MTOC; Chen & Chen, 2018; Swanson *et al*, 2019). In the spatiotemporal regulation of NLRP3 inflammasome activation, histone deacetylase 6 (HDAC6) reportedly promotes the transport of NLRP3 to the MTOC, where the NLRP3 inflammasome is activated (Magupalli *et al*, 2020). HDAC6 is a member of the class II deacetylase superfamily containing two active catalytic domains and a ubiquitin-binding domain (Grozinger *et al*, 1999; Verdel & Khochbin, 1999). HDAC6 is mainly localized in the cytoplasm and mediates the deacetylation of tubulin, resulting in the regulation of microtubule dynamics. By interacting with both ubiquitinated proteins and with the dynein motor complex, HDAC6 regulates the transfer of protein aggregates toward the MTOC, where aggresome formation takes place (Kawaguchi *et al*, 2003). However, the precise mechanisms whereby HDAC6 contributes to inflammasome activation are still unknown.

In this study, we found that the Ragulator complex expressed on the lysosomal membrane plays a critical role in inflammasome activation by interacting with HDAC6. We showed that myeloid-specific Lamtor1-deficient mice exhibited reduced *in vivo* inflammation caused by the administration of monosodium urate crystals (MSU) and alum, which activates the NLRP3 inflammasome. Of note, Lamtor1 deficiency in murine macrophages and human monocytic THP-1 cells abrogated NLRP3 and pyrin inflammasome activation but not the AIM2 inflammasome. Caspase-1 processing was impaired in Lamtor1-deficient BMDMs and THP-1 cells. Consistent with these results, the cleavage of GSDMD caused by inflammasome activation was reduced, resulting in pyroptosis impairment. Mechanistically, we found that the Ragulator complex interacted with HDAC6, which facilitated the interaction between the Ragulator complex and NLRP3, and that both interactions were required for the activation of the NLRP3 inflammasome. Moreover, by using a library of natural compounds to screen for inhibitors that blocked the interactions between Lamtor1 and HDAC6, we demonstrated that DL-all-rac- $\alpha$ -tocopherol, which is a synthetically produced form of vitamin E and not the natural form of D- $\alpha$ -tocopherol, reduced inflammasome activation. Finally, we also showed that DL-all-rac- $\alpha$ -tocopherol could alleviate acute gouty arthritis and peritonitis induced by MSU. Taken together, we have revealed that the Ragulator complex on the

lysosomal membrane plays a critical role in inflammasome activation *in vitro* and *in vivo* by interacting with NLRP3 via HDAC6, and that therapeutic applications targeting the interaction between the Ragulator complex and HDAC6 may be effective for IL-1 $\beta$ -related diseases.

## Results

### Lamtor1 is required for NLRP3 inflammasome activation in mice

The Ragulator complex has been shown to be involved in the differentiation of M2 macrophages and the regulation of the production of inflammatory cytokines, such as IL-6 and tumor necrosis factor- $\alpha$  (TNF- $\alpha$ ), by LPS stimulation (Kimura et al, 2016). However, the intraperitoneal administration of LPS resulted in a considerable decrease in serum IL-1 $\beta$  levels in myeloid cell-specific Lamtor1-deficient mice (*Lamtor1*<sup>fl $\alpha$ /fl $\alpha$</sup>  *LysM-Cre*; *LysM-Lamtor1*<sup>fl $\alpha$ /fl $\alpha$</sup>  mice; Fig EV1). The intraperitoneal injection of alum was found to cause IL-1 $\beta$  production via the NLRP3 inflammasome (Guarda et al, 2011). In *LysM-Lamtor1*<sup>fl $\alpha$ /fl $\alpha$</sup>  mice, this decreased the recruitment of leukocytes, including CD11b<sup>+</sup> Ly6G<sup>+</sup> neutrophils and CD11b<sup>+</sup> Ly6C<sup>+</sup> inflammatory monocytes, to the peritoneal cavity, and reduced IL-1 $\beta$  levels in peritoneal fluid when compared with WT mice (Fig 1A).

We further evaluated the role of Lamtor1 *in vivo* using a monosodium urate (MSU)-induced acute gouty arthritis model as the MSU crystals induced IL-1 $\beta$  production by NLRP3 inflammasome activation (Torres et al, 2009). After MSU crystals were injected into the tibia-tarsal joint, *LysM-Lamtor1*<sup>fl $\alpha$ /fl $\alpha$</sup>  mice showed significantly less ankle swelling than the WT mice (Fig 1B). Histopathological analysis showed that *LysM-Lamtor1*<sup>fl $\alpha$ /fl $\alpha$</sup>  mice exhibited a marked reduction in cellular infiltration in the ankle when compared to WT mice (Fig 1B). These results indicate that Lamtor1 is essential for the activation of the NLRP3 inflammasome *in vivo*.

### Lamtor1 is required for NLRP3 inflammasome activation *in vitro*

We next evaluated the *in vitro* biological effects of Lamtor1 in NLRP3 inflammasome activation. In addition to Lamtor1 deficient BMDMs, we generated the human monocytic cell line Lamtor1-KO THP-1 cells using the CrisprCas9 system to investigate the function of Lamtor1 in human cells (Fig EV1B; Nakatani et al, 2021). LPS priming followed by the administration of several NLRP3 inflammasome ligands, including nigericin, adenosine triphosphate (ATP), and the dipeptide glycyl-L-phenylalanine 2-naphthylamide (GPN), extremely reduced IL-1 $\beta$  release in the *LysM-Lamtor1*<sup>fl $\alpha$ /fl $\alpha$</sup>  bone marrow-derived macrophages (BMDMs; Fig 1C). Additionally, in THP-1 cells, more than 5 Lamtor1-KO single clones were obtained and

**Figure 1. NLRP3 inflammasome activation is impaired in myeloid-specific Lamtor1 deficiency.**

- A Effects of myeloid-specific Lamtor1 deficiency on peritoneal IL-1 $\beta$  production, CD11b<sup>+</sup> Ly6C<sup>+</sup> monocyte recruitment, and CD11b<sup>+</sup> Ly6G<sup>+</sup> neutrophil recruitment after an intraperitoneal injection of 600  $\mu$ l alum solution (20 mg/ml, 6 h). Data are shown as means  $\pm$  SEM. \* $P$  < 0.05 and \*\*\* $P$  < 0.001 by the Student's *t*-test,  $n$  = 6 mice (peritoneal IL-1 $\beta$  production) and 4 mice (FACS analysis).
- B Effects of myeloid-specific Lamtor1 deficiency in an acute gouty arthritis model. MSU crystals (0.5 mg) or the PBS control were injected intra-articularly into the tibia-tarsal joint of *Lamtor1*<sup>fl $\alpha$ /fl $\alpha$</sup>  and *Lamtor1*<sup>fl $\alpha$ /fl $\alpha$</sup>  *LysM-Cre* mice. Mice were assessed for joint swelling using electronic calipers. Images show photomicrographs (upper panel) and hematoxylin and eosin-stained sections (middle and lower panels) of ankle joints obtained at 24 h. Data are shown as the means  $\pm$  SEM. \*\*\* $P$  < 0.001 by the Student's *t*-test,  $n$  = 7 mice each. Scale bars = 50  $\mu$ m.
- C Effects of Lamtor1 deficiency on IL-1 $\beta$  secretion after NLRP3 inflammasome activation or TLR ligand stimulation. ELISA assay shows IL-1 $\beta$  secretion in supernatants from *Lamtor1*<sup>fl $\alpha$ /fl $\alpha$</sup>  and *Lamtor1*<sup>fl $\alpha$ /fl $\alpha$</sup>  *LysM-Cre* BMDMs treated with LPS (200 ng/ml, 4 h), followed by nigericin (15  $\mu$ M, 1 h), ATP (10 mM, 1 h), or GPN (100 nM, 6 h). Data are shown as the means  $\pm$  SEM. \* $P$  < 0.05 and \*\* $P$  < 0.01 by the Student's *t*-test,  $n$  = 3 biological replicates.
- D Effects of Lamtor1 deficiency on IL-1 $\beta$  secretion after NLRP3 inflammasome activation in human THP-1 monocytes. ELISA assay shows IL-1 $\beta$  secretion in supernatants from WT cells, Lamtor1 KO different single clones, all of which were treated with nigericin (15  $\mu$ M, 1 h) after priming with PMA (50 nM, overnight). Data are shown as the means  $\pm$  SEM. \*\*\* $P$  < 0.001 by one-way ANOVA,  $n$  = 3 biological replicates.
- E, F Effects of Lamtor1 deficiency on IL-1 $\beta$  secretion after the induction of endogenous ROS by mitochondrial poisons or the administration of an exogenous ROS (hydrogen peroxide). ELISA assay shows IL-1 $\beta$  secretion in supernatants after treatment with LPS (200 ng/ml), Rotenone (10  $\mu$ M), or Antimycin (10  $\mu$ g/ml) for 6 h or followed by hydrogen peroxide (3.86 mM). Data are shown as the means  $\pm$  SEM. \* $P$  < 0.05 and \*\*\* $P$  < 0.001 by the Student's *t*-test,  $n$  = 3 biological replicates.
- G Effects of Lamtor1 reconstitution in Lamtor1-deficient macrophages on IL-1 $\beta$  secretion after NLRP3 inflammasome activation. ELISA assay shows IL-1 $\beta$  secretion in BMDM supernatants from *Lamtor1*<sup>fl $\alpha$ /fl $\alpha$</sup>  cells, *Lamtor1*<sup>fl $\alpha$ /fl $\alpha$</sup>  *LysM-Cre* cells, and *Lamtor1*<sup>fl $\alpha$ /fl $\alpha$</sup>  *LysM-Cre* cells reconstituted with full-length Lamtor1, all of which were treated with nigericin (15  $\mu$ M, 1 h) after priming with LPS (200 ng/ml, 4 h). Data are shown as the means  $\pm$  SEM. \* $P$  < 0.05 and \*\* $P$  < 0.01 by one-way ANOVA,  $n$  = 3 biological replicates.
- H Effects of Lamtor1 deficiency on IL-1 $\beta$  secretion after NLRP3 inflammasome activation in human THP-1 monocytes. ELISA assay shows IL-1 $\beta$  secretion in supernatants from WT cells, Lamtor1 KO cells, and Lamtor1 KO cells reconstituted with full-length Lamtor1, all of which were treated with nigericin (15  $\mu$ M, 1 h) after priming with PMA (50 nM, overnight) and LPS (200 ng/ml, 2 h). Data are shown as the means  $\pm$  SEM. \*\*\* $P$  < 0.001 by one-way ANOVA,  $n$  = 3 biological replicates.
- I Effects of Lamtor1 deficiency on IL-18 secretion after NLRP3 inflammasome activation in human THP-1 monocytes. ELISA assay shows IL-18 secretion in supernatants from WT cells, Lamtor1 KO cells, and Lamtor1 KO cells reconstituted with full-length Lamtor1, all of which were treated with nigericin (15  $\mu$ M, 1 h) after priming with PMA (50 nM, overnight) and LPS (200 ng/ml, 2 h). Data are shown as the means  $\pm$  SEM. \*\*\* $P$  < 0.001 by one-way ANOVA,  $n$  = 3 biological replicates.
- J Effects of Lamtor1 deficiency on IL-1 $\beta$  secretion after P2X6 inflammasome activation. ELISA assay showing IL-1 $\beta$  secretion in supernatants from *Lamtor1*<sup>fl $\alpha$ /fl $\alpha$</sup>  and *Lamtor1*<sup>fl $\alpha$ /fl $\alpha$</sup>  *LysM-Cre* BMDMs treated with TcdB (0.5  $\mu$ g/ml, 3 h) after LPS (200 ng/ml, 4 h) stimulation. Data are shown as the means  $\pm$  SEM. \*\* $P$  < 0.01 no significant difference by one-way ANOVA,  $n$  = 3 biological replicates.
- K Effects of Lamtor1 deficiency on IL-1 $\beta$  secretion after AIM2 inflammasome activation. ELISA assay showing IL-1 $\beta$  secretion in supernatants from *Lamtor1*<sup>fl $\alpha$ /fl $\alpha$</sup>  and *Lamtor1*<sup>fl $\alpha$ /fl $\alpha$</sup>  *LysM-Cre* BMDMs treated with Poly(dA:dT; 5  $\mu$ g/ml, overnight) and Lipofectamine 3000 after LPS (200 ng/ml, 4 h) stimulation. Data information: Data are shown as the means  $\pm$  SEM. n.s no significant difference by one-way ANOVA,  $n$  = 3 biological replicates.

Source data are available online for this figure.

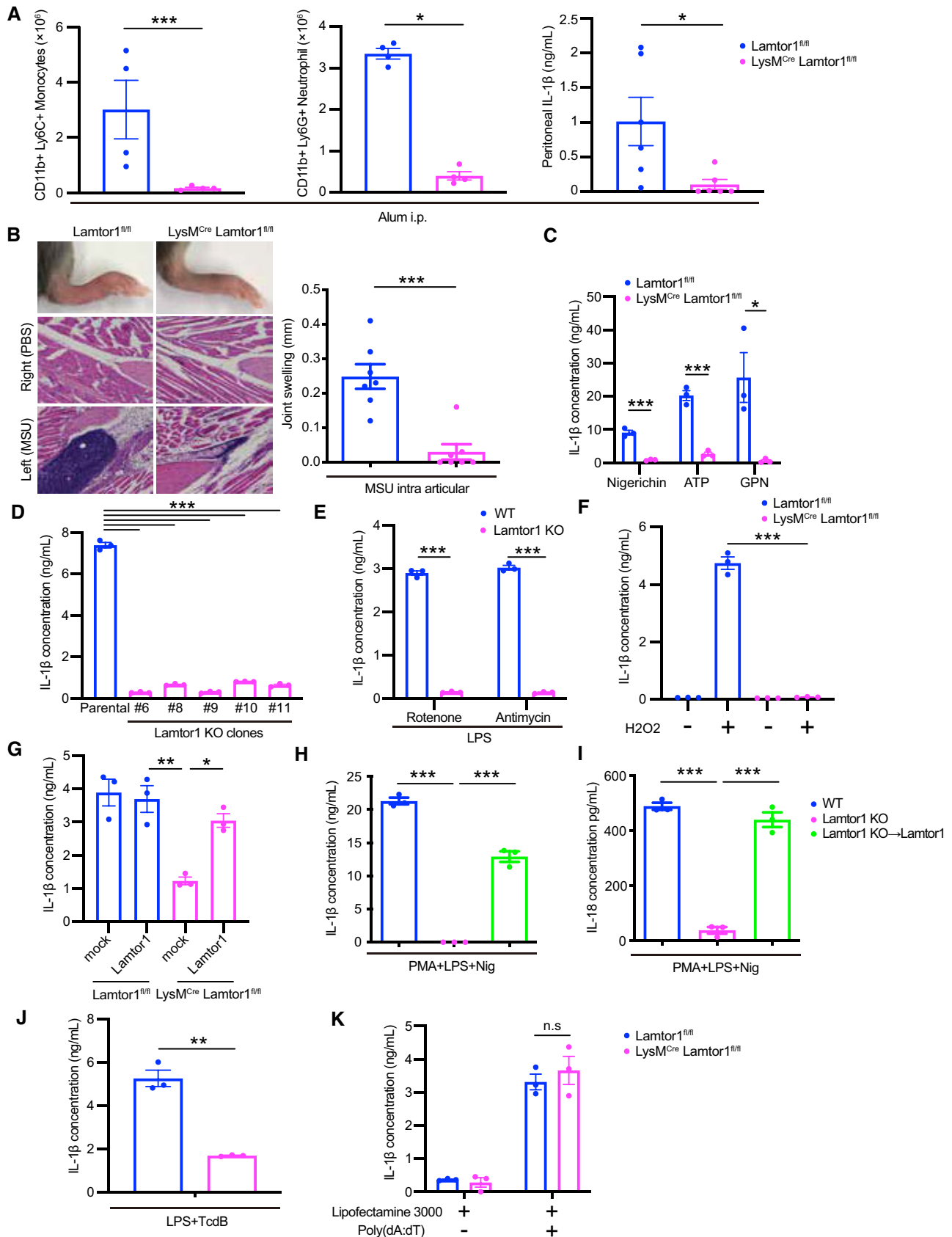


Figure 1.

every clone showed impaired IL-1 $\beta$  release in response to LPS priming and NLRP3 inflammasome stimuli (Fig 1D). However, toll-like-receptor (TLR) ligand-induced production of IL-6 was elevated in Lamtor1-deficient BMDMs (Fig EV1C; Kimura *et al*, 2016; Hayama *et al*, 2018). IL-1 $\beta$  release was also impaired in Lamtor1 deficient macrophages due to the induction of endogenous ROS in response to mitochondrial poisons or the administration of exogenous ROS such as hydrogen peroxide, both of which activate the NLRP3 inflammasome activator (Fig 1E and F; Sorbara & Girardin, 2011). Additionally, re-expression of the exogenous Lamtor1 protein by lentiviral transduction restored IL-1 $\beta$  secretion in response to inflammasome activation in Lamtor1-deficient BMDMs and Lamtor1-KO THP-1 cells (Figs 1G and H, and EV1D). The release of IL-18 was also significantly reduced in Lamtor1-KO THP-1 cells and rescued by the re-expression of exogenous Lamtor1 (Fig 1I). Furthermore, TcdB-induced Pyrin inflammasome activation was impaired in Lamtor1-deficient BMDMs (Fig 1J). By contrast, Poly(dA:dT)-induced AIM2 inflammasome was not suppressed in Lamtor1-deficient BMDMs (Fig 1K). These results suggest that Lamtor1 is essential for the activation of the NLRP3 inflammasome and pyrin inflammasome but not the AIM2 inflammasome.

### NLRP3 inflammasome activation is impaired in Lamtor1-deficient macrophages

We then examined which steps of inflammasome activation are affected by a Ragulator complex deficiency. As expected, pro-caspase-1 processing was significantly inhibited in Lamtor1-deficient BMDMs and Lamtor1 KO THP-1 cells (Fig 2A and B). Furthermore, the cleavage of GSDMD upon NLRP3 inflammasome activation was also reduced, resulting in the impairment of pyroptosis (Fig 2C and D). Since the pore formation of GSDMD is essential in IL-1 $\beta$  secretion (Shi *et al*, 2015; Sborgi *et al*, 2016), we considered the possibility that the mature form of IL-1 $\beta$  may be accumulated intracellularly. However, the mature form of IL-1 $\beta$  was not detected

in the cell lysate, and the reduced IL-1 $\beta$  release was not rescued by the lentiviral transduction of the activated form of GSDMD (Fig 2E–G). These results indicate that the dysregulation of GSDMD alone cannot explain the reduction in IL-1 $\beta$  release in Lamtor1 deficient macrophages. For the priming phase, protein synthesis after LPS stimulation was not impaired, except for pro-IL-1 $\beta$  in Lamtor1 deficient BMDMs (Fig 2H). However, the amount of IL-1 $\beta$  released did not catch up even when an excessive amount of IL-1 $\beta$  was exogenously expressed (Fig 2I). The mature form of IL-1 $\beta$  that was released was only rescued when the activated form of Caspase-1 (p10 and p20) was transduced in addition to the transduction of IL-1 $\beta$  (Fig 2I). Taken together, Lamtor1 was found to be essential for NLRP3 inflammasome activation.

### mTORC1 activity is not involved in the inflammasome activation phase

Next, we investigated the molecular mechanism of NLRP3 inflammasome activation by Lamtor1. Since the palmitoylation of the N-terminal region, the G2 of Lamtor1 is responsible for retaining Lamtor1 on lysosomal membranes (Nada *et al*, 2009), we investigated the importance of the localization of Lamtor1 on the lysosome by generating variants of Lamtor1 in which G2 was replaced with alanine (G2A). The G2A-mutant Lamtor1 was transduced into Lamtor1-KO THP-1 cells, but IL-1 $\beta$  production was not restored (Fig 3A and B), suggesting that the anchoring of Lamtor1 on the lysosomal membrane is crucial for inflammasome activation. Our first hypothesis was thus that reduced mTOR activity in Lamtor1 KO macrophages could affect the activation of the NLRP3 inflammasome (Fig 3C; Kimura *et al*, 2016). Pretreatment with rapamycin (mTORC1 inhibitor) before being stimulated with LPS plus nigericin reduced IL-1 $\beta$  production; however, the reduction due to the pretreatment with rapamycin was slight when compared to the IL-1 $\beta$  reduction in the Lamtor1 KO macrophages (Fig 3D). Moreover, when LPS was added first and then followed by rapamycin

**Figure 2. NLRP3 inflammasome activation is impaired in Lamtor1-deficient macrophages.**

- A, B Effects of Lamtor1 deficiency on Caspase-1 processing after NLRP3 inflammasome activation. Western blot shows caspase-1/p10, pro-caspase-1, Lamtor1, and  $\beta$ -actin. *Lamtor1*<sup>flox/flox</sup> and *Lamtor1*<sup>flox/flox</sup> *LysM-Cre* BMDMs (A) or WT and Lamtor1 KO THP-1 cells (B) were treated with nigericin (15  $\mu$ M, 1 h) after LPS [200 ng/ml, for 4 h (BMDM) or 2 h (THP-1)] stimulation. Data are shown as the means  $\pm$  SEM. \*\*\* $P$  < 0.001 by the Student's *t*-test,  $n$  = 3 biological replicates.
- C Effects of Lamtor1 deficiency on GSDMD processing after NLRP3 inflammasome activation. Western blot shows GSDMD, Lamtor1, and  $\beta$ -actin. *Lamtor1*<sup>flox/flox</sup> and *Lamtor1*<sup>flox/flox</sup> *LysM-Cre* BMDMs were treated with nigericin (15  $\mu$ M, 1 h) after LPS (200 ng/ml, 4 h) stimulation. Data are shown as the means  $\pm$  SEM. \* $P$  < 0.05 by the Student's *t*-test,  $n$  = 3 biological replicates.
- D Effects of Lamtor1 deficiency on pyroptosis after NLRP3 inflammasome activation. *Lamtor1*<sup>flox/flox</sup> and *Lamtor1*<sup>flox/flox</sup> *LysM-Cre* BMDMs were treated with nigericin (15  $\mu$ M, 1 h) after LPS (200 ng/ml, 4 h) stimulation, and the percentage of propidium iodide positive cells was counted by flow cytometry. Data are shown as the means  $\pm$  SEM. \*\*\* $P$  < 0.001 by the Student's *t*-test,  $n$  = 3 biological replicates.
- E Effects of Lamtor1 deficiency on IL-1 $\beta$  dynamics. Western blot shows IL-1 $\beta$  and  $\beta$ -actin. WT cells and Lamtor1 KO cells were treated with nigericin (15  $\mu$ M, 1 h) after priming with PMA (50 nM, overnight) stimulation.
- F Effects of the active form of GSDMD reconstitution on Lamtor1 KO THP-1 cells. ELISA assay shows IL-1 $\beta$  secretion in supernatants from WT cells, Lamtor1 KO cells, and Lamtor1 KO cells reconstituted with the active form of GSDMD, all of which were treated with nigericin (15  $\mu$ M, 1 h) after priming with PMA (50 nM, overnight) and LPS (200 ng/ml, 2 h). Data are shown as means  $\pm$  SEM. n.s. indicates  $P$  > 0.05 by one-way ANOVA,  $n$  = 3 biological replicates.
- G Confirmation of the reconstitution of the active form Caspase-1 (p10 and p20) or GSDMD (GSDMD-NT).
- H Effects of Lamtor1 deficiency on the priming phase. *Lamtor1*<sup>flox/flox</sup> and *Lamtor1*<sup>flox/flox</sup> *LysM-Cre* BMDMs were treated with LPS (200 ng/ml, 4 h). Data are shown as the means  $\pm$  SEM. \*\*\* $P$  < 0.001 by the Student's *t*-test,  $n$  = 3 biological replicates.
- I Effects of IL-1 $\beta$  and active form of Caspase-1 reconstitution on Lamtor1 KO THP-1 cells. ELISA assay shows IL-1 $\beta$  secretion in supernatants from WT cells, Lamtor1 KO cells, and Lamtor1 KO cells reconstituted with IL-1 $\beta$ , the active form of Caspase-1, all of which were treated with nigericin (15  $\mu$ M, 1 h) after priming with PMA (50 nM, overnight) and LPS (200 ng/ml, 2 h). Data are shown as the means  $\pm$  SEM. \*\*\* $P$  < 0.001 by the Student's *t*-test and n.s. indicates  $P$  > 0.05 by one-way ANOVA,  $n$  = 3 biological replicates.

Source data are available online for this figure.

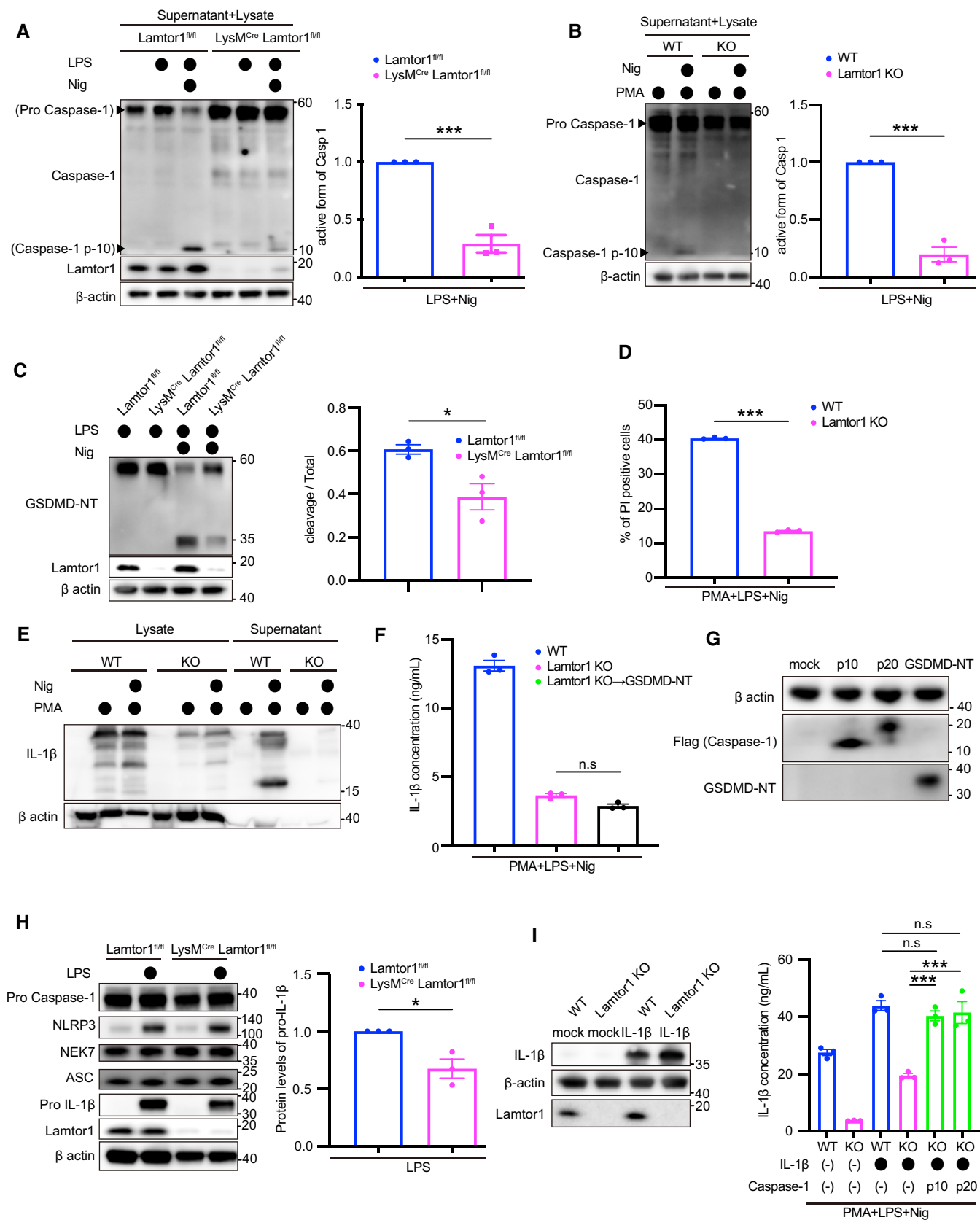


Figure 2.

treatment to avoid the effect of rapamycin priming, Caspase-1 processing was not affected (Fig 3E). IL-1 $\beta$  production was not affected by the Torin-1 treatment (mTORC1/mTORC2 inhibitor; Fig 3F). These results indicate that the NLRP3 inflammasome activation phase is independent of mTORC1 activity.

We have previously reported that the loss of Lamtor1 promotes the nuclear translocation of the transcription factor EB (TFEB), the master regulator of the lysosomal biogenesis (Sardiello et al, 2009), and autophagy (Sardiello et al, 2009), resulting in increased LC3 expression, which is a standard marker for autophagosomes (Hayama et al, 2018). Therefore, we generated myeloid cell-specific Lamtor1/TFEB double-knockout mice to investigate whether the decrease in NLRP3 inflammasome activity in the Lamtor1-KO cells was caused by enhanced TFEB nuclear translocation (Figs 2B and EV2A). However, the level of IL-1 $\beta$  production by the Lamtor1/TFEB double-KO BMDMs upon LPS plus nigericin stimulation was similar to that by Lamtor1-KO BMDMs (Fig EV2C). These results indicate that the decrease in IL-1 $\beta$  production in Lamtor1-deficient macrophages was independent of TFEB nuclear localization.

### Lamtor1 interacts with HDAC6

Since Lamtor1 must be present on the lysosome to be involved in NLRP3 inflammasome activation, and since its action is not through mTORC1 pathways, we searched for proteins with which Lamtor1 interacts on the lysosome. Lysosomes of THP-1 cells were isolated using a concentration gradient method to perform quantitative proteomics and thereby screen for proteins mobilized to the lysosomes upon LPS stimulation. Of the many proteins mobilizing to the lysosomes after the LPS treatment, we focused on HDAC6, as the phenotype of Lamtor1-KO BMDMs was shown to be similar to that of HDAC6-KO BMDMs as the NLRP3 and pyrin inflammasomes were impaired, but AIM2 inflammasome response intact (Magupalli et al, 2020; Fig 1J and K). Consistent with the aforementioned study, the activation of the NLRP3 inflammasome in BMDMs was reduced with the HDAC6 inhibitor treatment (Fig 4A). We thus investigated whether the interaction of Lamtor1 with HDAC6 was required for Lamtor1-mediated IL-1 $\beta$  production. Lamtor1 and HDAC6 were co-immunoprecipitated in HEK293T cells that stably expressed myc-

tagged HDAC6 (HDAC6-myc-HEK293T) and FLAG-tagged Lamtor1 (Lamtor1-FLAG; Fig 4B and C). To confirm the interaction between endogenous Lamtor1 and endogenous HDAC6, we established Lamtor1-Flag knocked-in THP-1 cells (Lamtor1-FLAG KI). The interaction between Lamtor1 and endogenous HDAC6 was confirmed in Lamtor1-FLAG KI cells (Fig 4D). We further confirmed the co-immunoprecipitation of endogenous Lamtor1 and HDAC6 in LPS-treated THP-1 WT cells, suggesting that this interaction occurred in physiological conditions (Fig 4E). Moreover, Lamtor1 and HDAC6 interactions were enhanced by LPS stimulation (Fig 4F). We then examined the interaction of Lamtor1 and HDAC6 in living cells by performing an *in situ* proximity ligation assay (PLA), and a NanoLuc luciferase-based bioluminescence resonance energy transfer (NanoBRET) assay. Endogenous HDAC6 was present in close proximity to endogenous Lamtor1 after stimulation with LPS plus nigericin (Fig 4G), and BRET occurred between Lamtor1 and HDAC6 (Fig 4H). From these experiments, we revealed that Lamtor1-HDAC6 interactions occurred in single living cells. Furthermore, to identify the essential region for the interaction between HDAC6 and Lamtor1, we investigated the interactions between HDAC6 and a truncated form of Lamtor1 ( $\Delta$ 145–161, Met1-Ser144;  $\Delta$ 95–161, Met1-Val94). Lamtor1 $^{\Delta$ 145–161 interacted with HDAC6, but Lamtor1 $^{\Delta$ 95–161 did not (Fig 4I), suggesting that the region of Lamtor1 from amino acids 95–144, where alpha 3 and alpha 4 helices are located, is essential for interactions with HDAC6. Consistent with this, the restoration of Lamtor1 $^{\Delta$ 95–161 in Lamtor1-KO THP-1 cells failed to rescue the reduction of IL-1 $\beta$  production in Lamtor1-KO THP-1 cells (Fig 4J). These results indicate that the interaction of Lamtor1 and HDAC6 on the lysosomal membrane is important for the activation of the NLRP3 inflammasome.

### Lamtor1 interacts with NLRP3 in the presence of HDAC6

HDAC6 reportedly transports the NLRP3 inflammasome to the MTOC (Magupalli et al, 2020) and interacts with NLRP3 (Hwang et al, 2015). We therefore examined whether the NLRP3 inflammasome component was mobilized to lysosomes by LPS and nigericin stimulation and whether the interaction between Lamtor1 and HDAC6 was important for NLRP3 inflammasome activation. We

#### Figure 3. mTORC1 activity is not involved in the inflammasome activation phase.

- A Representative images of mutant Lamtor1. PMA-primed Lamtor1 KO THP-1 macrophages reconstituted with full-length or truncated Lamtor1. Scale bars = 5  $\mu$ m.
- B Effects of the Lamtor1 point mutation on IL-1 $\beta$  secretion after NLRP3 inflammasome activation. ELISA assays show IL-1 $\beta$  secretion in THP-1 cell supernatants from WT cells, Lamtor1 KO cells, and Lamtor1 KO cells reconstituted with full-length Lamtor1 or variants of Lamtor1 in which G2 was replaced with alanine (G2A); all cell types were then treated with nigericin (15  $\mu$ M, 1 h) after priming with PMA (50 nM, overnight). Data are shown as the means  $\pm$  SEM. \* $P$  < 0.05 and \*\*\* $P$  < 0.001 by one-way ANOVA,  $n$  = 3 biological replicates.
- C Effects of Lamtor1 deficiency on mTORC1 activity. Immunoblot analysis of Lamtor1 $^{fllox/fllox}$  and Lamtor1 $^{fllox/fllox}$  *LysM-Cre* BMDMs treated with LPS (200 ng/ml, 4 h).
- D Effect of the rapamycin treatment on IL-1 $\beta$  secretion after NLRP3 inflammasome activation. ELISA assay shows IL-1 $\beta$  secretion in supernatants from PMA (50 nM, overnight) primed WT THP-1 cells treated with rapamycin at the indicated concentration for 2 h, then treated with LPS (200 ng/ml, 2 h) and nigericin (15  $\mu$ M, 1 h). Data are shown as the means  $\pm$  SEM. \*\* $P$  < 0.01, and n.s indicates no significant difference by one-way ANOVA,  $n$  = 3 biological replicates.
- E Effect of rapamycin treatment on Caspase-1 processing. Western blot shows caspase-1/p20. LPS (200 ng/ml, 4 h) primed BMDMs were treated with rapamycin at indicated concentrations followed by nigericin (15  $\mu$ M, 1 h). Data are shown as the means  $\pm$  SEM. n.s indicates no significant difference by one-way ANOVA,  $n$  = 3 biological replicates.
- F Effect of Torin-1 treatment on IL-1 $\beta$  secretion after NLRP3 inflammasome activation. ELISA assay shows IL-1 $\beta$  secretion in supernatants from WT BMDMs pretreated with Torin-1 (0, 1, 10, 100, or 250 nM) for 2 h before LPS (200 ng/ml, 4 h) and nigericin (15  $\mu$ M, 1 h) treatment (left panel). Western blot shows phospho-p70-S6K from BMDMs pretreated with Torin-1 at the indicated concentrations for 2 h before LPS and nigericin treatment (right panel). Data are shown as the means  $\pm$  SEM. n.s indicates no significant difference by one-way ANOVA,  $n$  = 3 biological replicates.

Source data are available online for this figure.

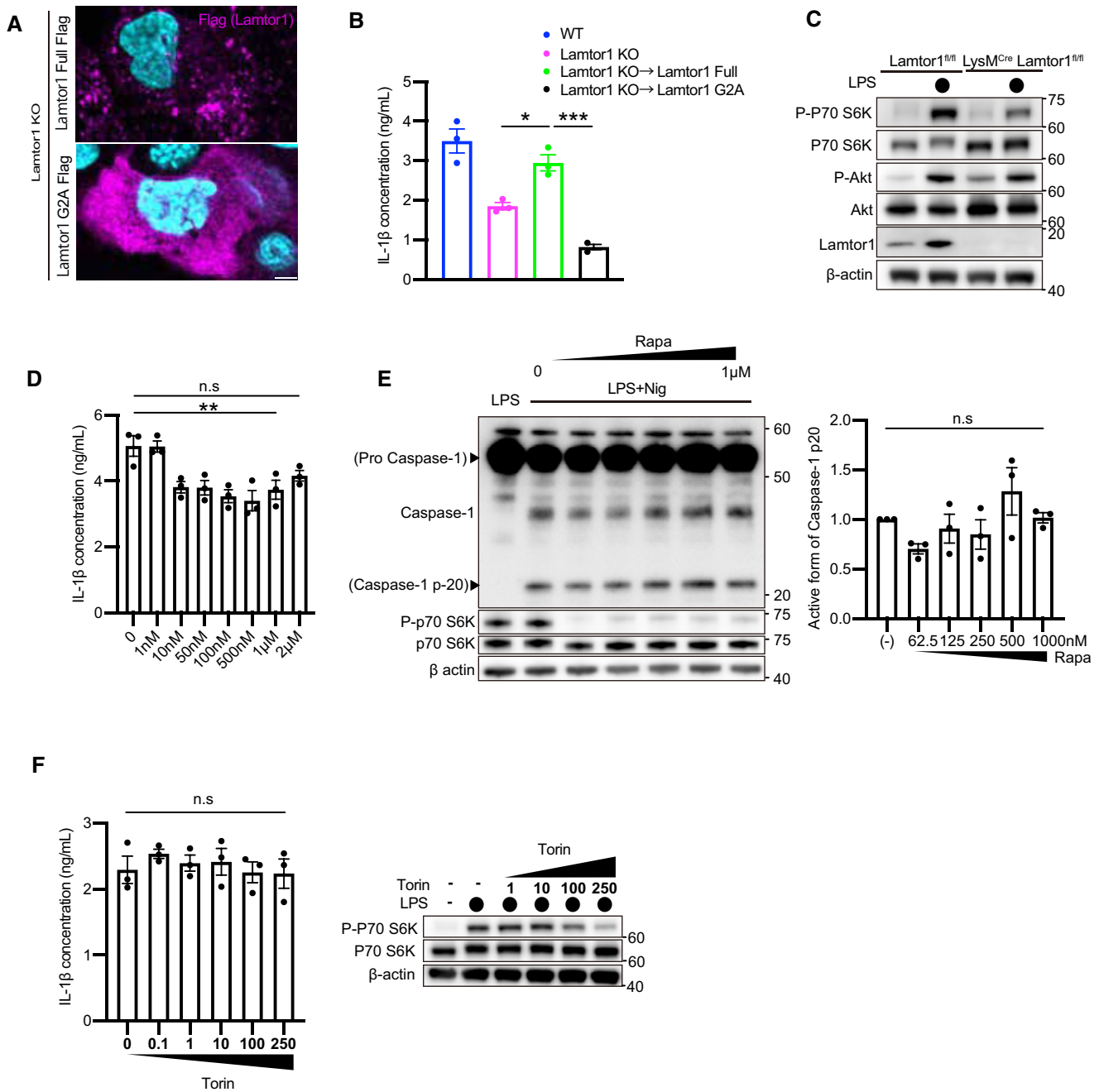


Figure 3.

first revealed the Lamtor1 bound NLRP3 using a yeast two-hybrid system (Fig 5A). Then, to examine whether endogenous Lamtor1 interacts with endogenous NLRP3 in living cells, we performed PLA using anti-Flag and anti-NLRP3 antibodies in Lamtor1-FLAG KI cells. NLRP3 was found to be proximal to Lamtor1 following stimulation with LPS and nigericin (Fig 5B). Additionally, Lamtor1 and NLRP3 were co-immunoprecipitated with each other (Fig 5C and D). Then, to identify whether the complete Ragulator complex formation is necessary for this interaction, we introduced the Lamtor1 <sup>$\Delta$ 145-161</sup> mutant (Met1-Ser144) into HEK293T cells that stably

expressed NLRP3-Flag as the Lamtor1 <sup>$\Delta$ 145-161</sup> mutant cannot form the Ragulator complex (Nakatani *et al*, 2021). The interaction between NLRP3 and Lamtor1 <sup>$\Delta$ 145-161</sup> was significantly reduced when compared with the interactions between NLRP3 and the full-length Lamtor1 (Fig 5E and F). This suggests that the complete formation of the Ragulator complex is required for binding to NLRP3. Furthermore, when HDAC6 expression was interfered with by shRNA, the interaction between Lamtor1 and NLRP3 was reduced (Fig 5G). These results indicate that HDAC6 promotes the interaction between Lamtor1 and NLRP3.



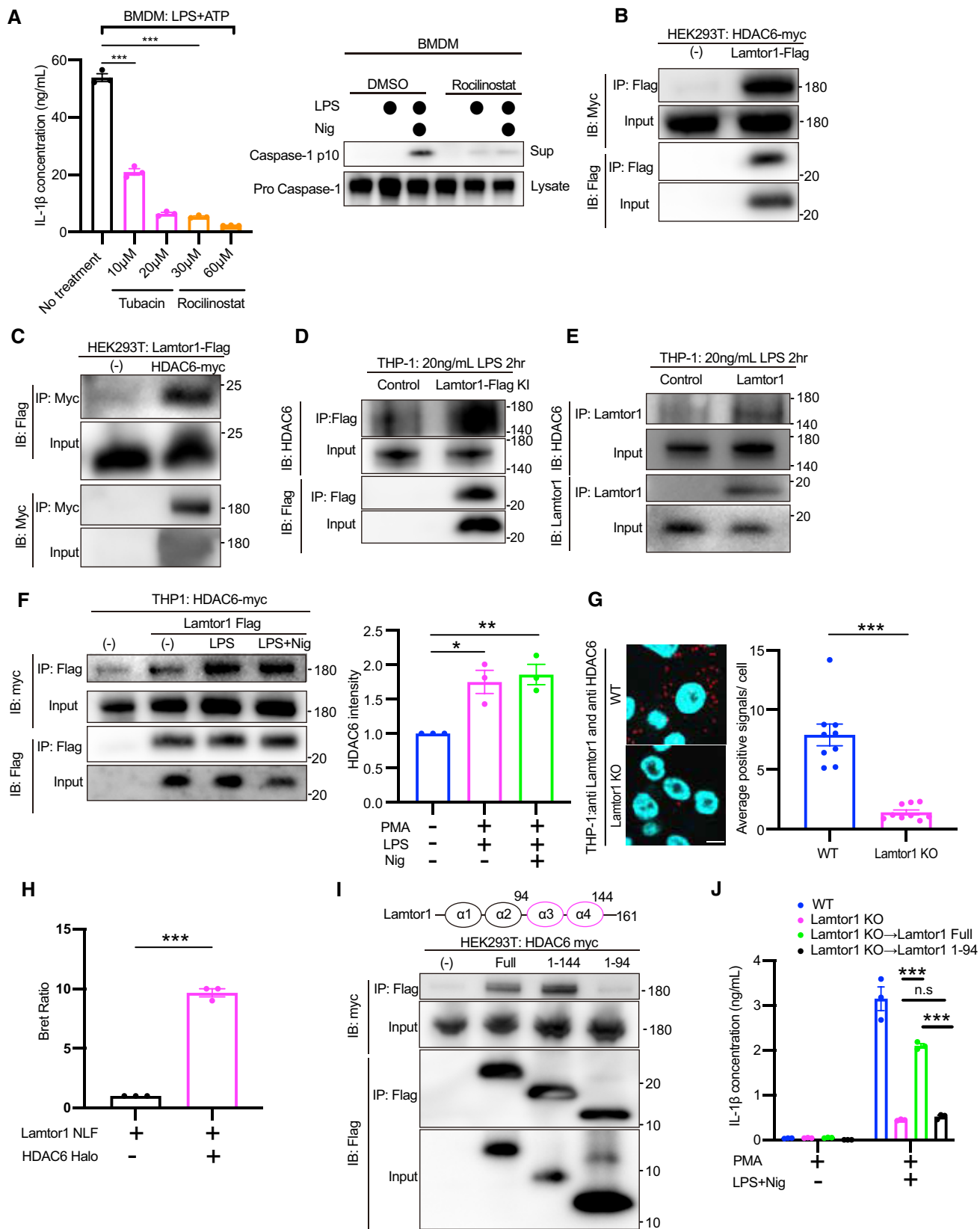


Figure 4.

**Figure 4. Interaction between Lamtor1 and HDAC6 is necessary for inflammasome activation.**

- A Effects of the HDAC6 inhibitor treatment on IL-1 $\beta$  secretion after NLRP3 inflammasome activation. ELISA assays show IL-1 $\beta$  secretion and caspase-1 processing (p10) in BMDMs upon NLRP3 inflammasome activation following pretreatment with tubacin (left to right: 10 and 20 mM) or rocilinostat (left to right: 30 and 60 mM). Data are shown as the means  $\pm$  SEM. \*\*\* $P$  < 0.001 by one-way ANOVA,  $n$  = 3 biological replicates.
- B–F Co-immunoprecipitation assay showing the interaction between Lamtor1 and HDAC6. Immunoblot analysis of Lamtor1–Flag co-immunoprecipitated with HDAC6–myc from lysates of HEK293T cells transfected with the indicated plasmids (B, C), Lamtor1–Flag co-immunoprecipitated with endogenous HDAC6 from the lysate of Lamtor1–Flag knocked-in THP-1 cells. (D) Endogenous Lamtor1 co-immunoprecipitated with endogenous HDAC6 from lysates of WT THP-1 cells (E, F). Effects of NLRP3 inflammasome activation on the interactions between Lamtor1 and HDAC6. Co-immunoprecipitation assay shows interactions between Lamtor1 and HDAC6. Immunoblot analysis of Lamtor1–Flag co-immunoprecipitated with HDAC6–myc from lysates of HEK293T cells transfected with the indicated plasmids. Data are shown as means  $\pm$  SEM. \* $P$  < 0.05 and \*\* $P$  < 0.01 by one-way ANOVA,  $n$  = 3 biological replicates.
- G PLA to confirm endogenous binding between Lamtor1 and HDAC6. Lamtor1–HDAC6 complexes are shown in red, and nuclei are depicted in blue. *In situ* PLA signals were quantified over nine images in each experiment. Data are shown as the means  $\pm$  SEM. \*\*\* $P$  < 0.001 by the Student's  $t$ -test. The data are representative of three experiments that showed consistent results. Scale bars, 10  $\mu$ m.
- H NanoBRET assay to confirm endogenous binding between Lamtor1 and HDAC6 in living cells. HEK293T cells were transiently transfected with NanoLuc-fused Lamtor1 and HaloTag-fused HDAC6 using Lipofectamine 2000. Luminescence was measured 48 h after transfection following the addition of Nano-Glo Luciferase Assay Substrate (Promega). Data are shown as the means  $\pm$  SEM. \*\*\* $P$  < 0.001 by the Student's  $t$ -test,  $n$  = 3 biological replicates.
- I Immunoblot analysis of the truncated form of Flag-tagged Lamtor1 mutant ( $\Delta$ 145–161, Met1–144;  $\Delta$ 95–161, Met1–Val194) co-immunoprecipitated with HDAC6–myc from lysates of HEK293T cells transfected with the indicated plasmids.
- J Effect of truncated Lamtor1 mutant on NLRP3 inflammasome activation in THP-1 cells. ELISA assay showing IL-1 $\beta$  secretion in supernatants from WT cells, Lamtor1 KO cells, Lamtor1 KO cells reconstituted with full-length Lamtor1, and Met1–Val194 Lamtor1 cells; all cell types were treated with nigericin (15  $\mu$ M, 1 h) after priming with PMA (50 nM, overnight). Data are shown as the means  $\pm$  SEM. \*\*\* $P$  < 0.001 and n.s. indicates no significant difference by the Student's  $t$ -test,  $n$  = 3 biological replicates.

Source data are available online for this figure.

**ASC specks originate near the lysosomes**

To verify that Lamtor1 functions in the activation phase of the NLRP3 inflammasome, we observed the localization of Lamtor1 at the moment of ASC speck formation using live cell imaging, which can be used as a simple upstream readout for inflammasome activation (Elliott & Sutterwala, 2015). We established stably expressing GFP-tagged ASC and tdTomato-tagged Lamtor1 THP-1 cells. After stimulation with nigericin, ASC specks rapidly formed and Lamtor1 was located near or at the center of the origin of ASC speck formation (Fig 6A and B; Movies EV1 and EV2). Moreover, ASC speck formation did not occur in GFP-tagged ASC-expressing Lamtor1 KO cells (Fig 6C). These results suggest that ASC specks originate near the lysosomes and that Lamtor1 takes part in the inflammasome activation phase.

**DL-all-rac- $\alpha$ -tocopherol inhibits Lamtor1 and HDAC6 interactions**

We subsequently attempted to identify the regulatory system responsible for the activation of the Lamtor1–HDAC6 interaction. Using the NanoBRET assay, we performed two rounds of screening using a library of natural compounds and identified DL-all-rac- $\alpha$ -tocopherol as a potent negative regulator that specifically modulates the interactions between Lamtor1 and HDAC6 (Fig 7A). To confirm that DL-all-rac- $\alpha$ -tocopherol attenuates the interaction between Lamtor1 and HDAC6, we performed co-immunoprecipitation assays. An immunoprecipitation assay revealed that the interaction between HDAC6 and Lamtor1 was reduced in the presence of DL-all-rac- $\alpha$ -tocopherol (Fig 7B). Treatment of the WT BMDMs with DL-all-rac- $\alpha$ -tocopherol dose-dependently decreased ATP-induced IL-1 $\beta$  release (Fig 7C). By contrast, DL-all-rac- $\alpha$ -tocopherol did not affect nuclear factor  $\kappa$ B-dependent priming as measured by IL-6 secretion or by protein synthesis related to NLRP3 inflammasome activation (Figs 7D and EV3A). Additionally, DL-all-rac- $\alpha$ -tocopherol administration did not inhibit the overall activity of HDAC6, as indicated by the acetylation of  $\alpha$ -tubulin (Fig EV3B). These data suggest that DL-

all-rac- $\alpha$ -tocopherol inhibits the interaction between HDAC6 and Lamtor1 independently of the catalytic activity of HDAC6.  $\alpha$ -tocopherol has three chiral centers in the phytyl tail, resulting in eight stereoisomeric forms (Burton & Traber, 1990). The synthetic form, DL-all-rac- $\alpha$ -tocopherol consists of approximately equal amounts of the eight possible stereoisomers, whereas naturally occurring  $\alpha$ -tocopherol exists only as the RRR-form (D- $\alpha$ -tocopherol; Burton & Traber, 1990; Ranard & Erdman, 2018). It is of note that the interaction between Lamtor1 and HDAC6 was not prohibited by D- $\alpha$ -tocopherol (Fig 7E). We compared the inhibitory effects on NLRP3 inflammasome activation and found that DL-all-rac- $\alpha$ -tocopherol suppressed ATP-induced IL-1 $\beta$  release more than D- $\alpha$ -tocopherol even though both DL-all-rac- $\alpha$ -tocopherol and D- $\alpha$ -tocopherol have antioxidant properties (Fig 7F; Hoppe & Krennrich, 2000). Taken together, DL-all-rac- $\alpha$ -tocopherol inhibits IL-1 $\beta$  release not only due to the antioxidant effects but also by blocking the interaction between Lamtor1 and HDAC6.

**DL-all-rac- $\alpha$ -tocopherol inhibits inflammasome activation in mice**

MSU-induced gouty arthritis and a peritonitis model were used to investigate whether DL-all-rac- $\alpha$ -tocopherol treatment effectively decreased IL-1 $\beta$  production *in vivo*. When MSU crystals with or without DL-all-rac- $\alpha$ -tocopherol were injected into the tibia-tarsal joints of mice, those treated with DL-all-rac- $\alpha$ -tocopherol showed significantly less swelling and cellular infiltration (Fig 7G). Consistent with this, DL-all-rac- $\alpha$ -tocopherol administration reduced inflammatory responses, as was indicated by the lower levels of cellular infiltration and IL-1 $\beta$  in the peritoneal fluid of the MSU-induced peritonitis model mice (Fig 7H). DL-all-rac- $\alpha$ -tocopherol did not affect cell migration although the Ragulator complex reportedly is implicated in the leukocyte trafficking (Fig EV3C). Collectively, these results indicate that the interactions between Lamtor1 and HDAC6 are necessary for NLRP3-inflammasome activation *in vivo*, and that DL-all-rac- $\alpha$ -tocopherol may improve the inflammation caused by inflammasome activation.

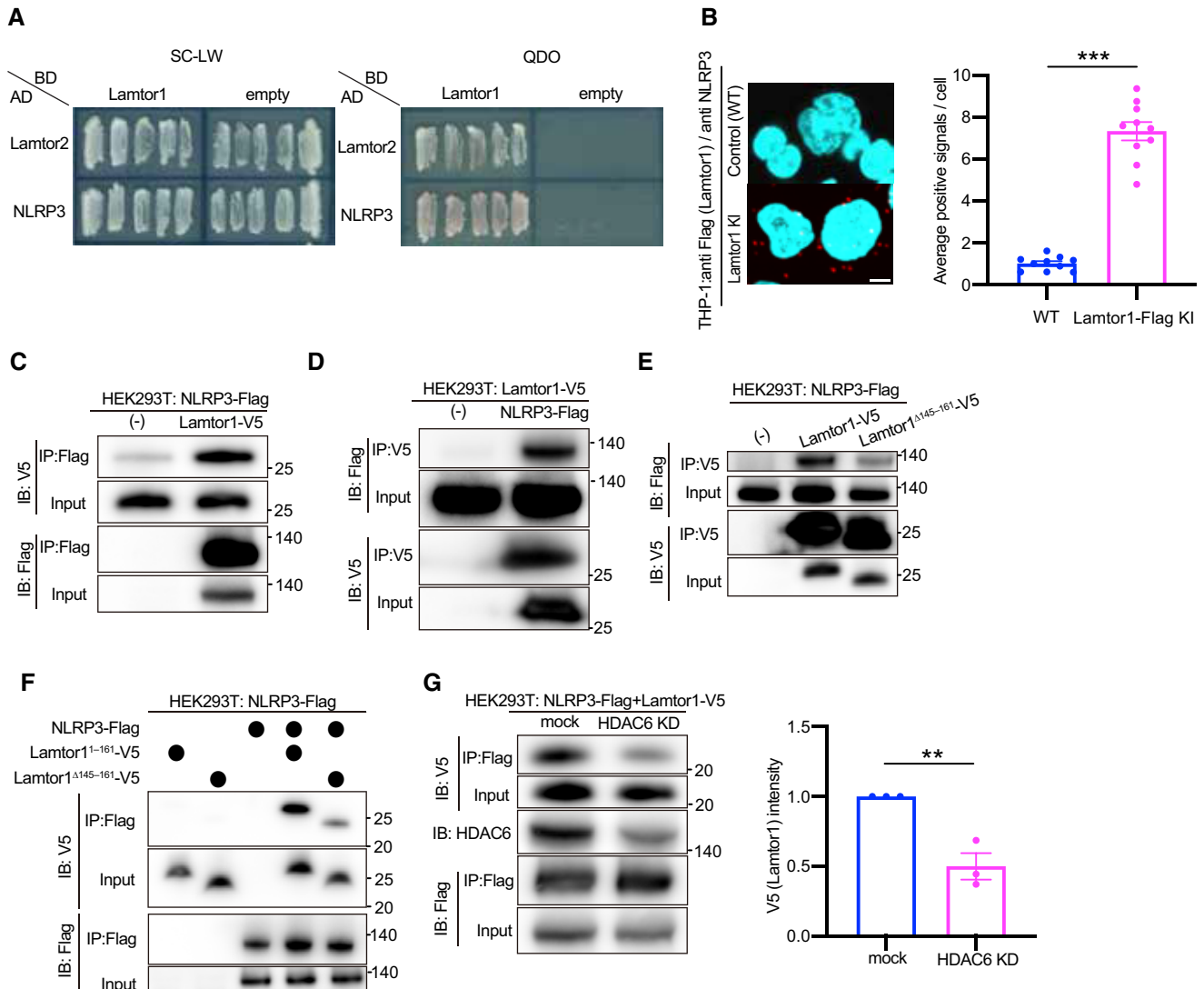


**Figure 5. Lamtor1 interacts with NLRP3 in the presence of HDAC6.**

- A** Yeast two-hybrid (Y2H) assays for Lamtor1 interactions with NLRP3. Positive Y2H interaction between Lamtor1 as prey, and NLRP3 as bait. Lamtor2 as prey was used as a positive control and the empty bait vector as a negative control.
- B** PLA to confirm endogenous binding between Lamtor1 and NLRP3. Lamtor1–NLRP3 complexes are shown in red, and nuclei are depicted in blue. *In situ* PLA signals were quantified over 10 images in each experiment. Data are shown as the means  $\pm$  SEM. \*\*\* $P < 0.001$  by the Student's *t*-test. The data are representative of three experiments that showed consistent results. Scale bars = 5  $\mu$ m.
- C, D** Immunoblot analysis of Lamtor1-V5 co-immunoprecipitated with NLRP3–Flag from lysates of HEK293T cells transfected with the indicated plasmids.
- E, F** Immunoblot analysis of the truncated form of V5-tagged Lamtor1 mutant ( $\Delta 145$ –161, Met1–Ser144) co-immunoprecipitated with NLRP3–flag from lysates of HEK293T cells transfected with the indicated plasmids.
- G** Effect of the HDAC6 knockdown on NLRP3–Lamtor1 interactions. Immunoblot analysis of Lamtor1–V5 co-immunoprecipitated with NLRP3–Flag from lysates of HEK293T cells transfected with the indicated plasmids. Data are shown as the means  $\pm$  SEM. \*\* $P < 0.01$  by the Student's *t*-test,  $n = 3$  biological replicates.

Source data are available online for this figure.

## Discussion

In this study, we found that the Ragulator complex expressed on the lysosomal membrane plays a critical role in NLRP3 inflammasome activation by interacting with HDAC6 (Fig 8). Myeloid-specific Lamtor1-deficient mice showed reduced inflammation in an acute gouty arthritis model and in both alum- and LPS-induced peritonitis

models. Additionally, Lamtor1 deficiency in murine macrophages and human monocytic THP-1 cells abrogated NLRP3 inflammasome activation. Lamtor1 interacted with HDAC6, which augments the interaction between Lamtor1 and NLRP3. Lamtor1 was located near or at the center of the origination of ASC speck formation. Moreover, by screening a library of natural compounds, we found that DL-all-rac- $\alpha$ -tocopherol, a synthetically produced form of vitamin E,

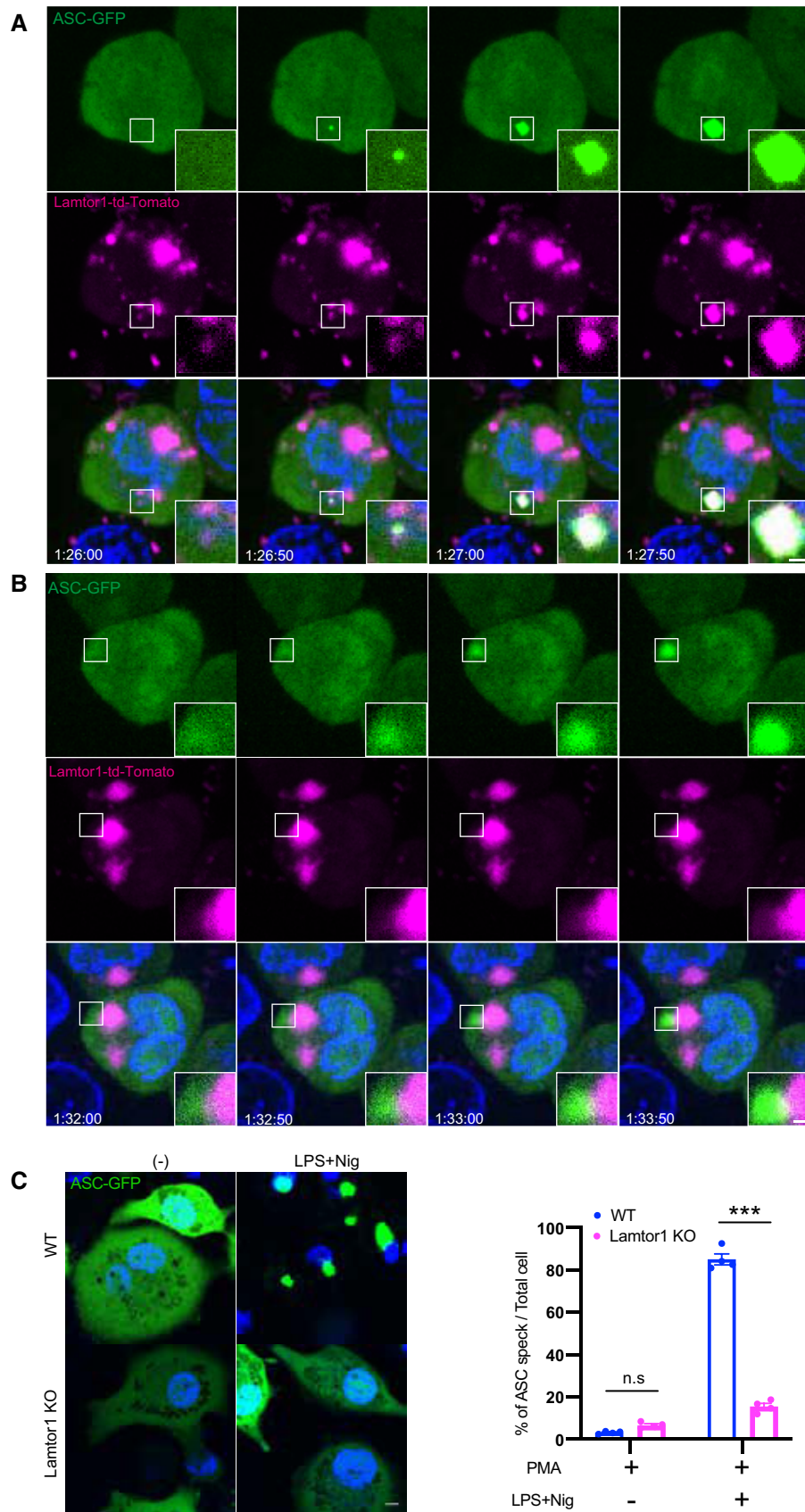


Figure 6.

**Figure 6. ASC speck originates near the lysosomes.**

- A, B Representative images of Lamtor1 and ASC. PMA-treated THP-1 cells stably expressing GFP-tagged ASC and tdTomato-tagged Lamtor1 were primed with LPS (200 ng/ml, 2 h) and then stimulated with nigericin for the indicated duration. Time shows after nigericin stimulation (min:s). Scale bars = 1  $\mu$ m.
- C Effects of Lamtor1 deficiency on ASC speck formation after NLRP3 inflammasome activation. Representative images of PMA-primed THP-1 macrophages stably expressing GFP-tagged ASC treated with or without LPS (200 ng/ml, 2 h) and nigericin (15  $\mu$ M, 1 h). Scale bars = 10  $\mu$ m. Data are shown as the means  $\pm$  SEM. \*\*\* $P$  < 0.001, and n.s indicates no significant difference by one-way ANOVA,  $n$  = 4 independent experiments.

Source data are available online for this figure.

but not D- $\alpha$ -tocopherol, inhibited the interactions between Lamtor1 and HDAC6 and reduced inflammasome activation. Finally, we showed that DL-all-rac- $\alpha$ -tocopherol alleviated acute gouty arthritis and MSU-induced peritonitis.

The question as to how inflammasome activation is regulated is very challenging, as their activation involves an elaborate process with a variety of regulators. To investigate the mechanisms of inflammasome activation, the priming, activation, and secretion phases are usually discussed separately for convenience, but their effector molecules and modifications can be interrelated in a series of steps. Therefore, it is not easy to determine which molecule is acting in which phase. Recently, Evavold *et al* (2021) suggested that the Ragulator complex promotes GSDMD oligomerization at the membrane but not caspase-1-mediated cleavage of GSDMD (Evavold *et al*, 2021). Zheng *et al* (2021) reported that the Ragulator complex is required for RIPK1-caspase-8-driven cell death, but it is not required for canonical or noncanonical inflammasome-induced signaling (Zheng *et al*, 2021). Both groups argue that the Ragulator complex is involved in the secretory phase but not the inflammasome activation phase. Actually, the Ragulator complex is involved in all steps of inflammasome activation, namely the priming, activation, and secretion phases. However, we have emphasized the role of the Ragulator complex in the activation phase as we have provided evidence for the involvement of the Ragulator complex in the inflammasome activation phase by exhibiting (i) reduced Caspase-1 processing in Lamtor1 deficient macrophages, (ii) restored IL-1 $\beta$  production in a rescue experiment for the active form of Caspase-1, and (iii) interactions between Lamtor1 and NLRP3 coordinated by HDAC6. Considering the implications of these interactions, it is reasonable to conclude that the Ragulator complex is involved in the inflammasome activation phase.

There are many possible reasons why our conclusions differ from theirs. For example, the selection of which genes are knocked out can be influential. As we have shown the importance of specific interactions between Lamtor1 and HDAC6 / NLRP3, especially the  $\alpha$ 3 and  $\alpha$ 4 helix of Lamtor1, which were required for interactions with HDAC6, and this means that different interfaces of the Ragulator complex are utilized between interactions with RagA/C and HDAC6 (Yonehara *et al*, 2017). Therefore, knockouts of the other Ragulator-Rag complex proteins such as RagA or RagC may not detect these functions. Moreover, the difference in the cells analyzed may be another reason. In this study, primary bone marrow-derived macrophages and human THP-1 cell lines were mainly used, whereas in previous studies, immortalized bone marrow-derived macrophage cell lines were used (Evavold *et al*, 2021; Zheng *et al*, 2021). Whatever the cause, it is of note that every report including this one has consistently confirmed that the Ragulator complex positively regulates inflammasome activity in terms of IL-1 $\beta$  release or pyroptosis when cells are exposed to cellular stress.

Recently, several groups stated that the Ragulator complex controls GSDMD pore formation through several mechanisms, including the regulation of ROS production, which results in GSDMD oxidation and oligomerization (Evavold *et al*, 2021; Zheng *et al*, 2021; preprint: Devant *et al*, 2022). In this study, IL-1 $\beta$  release reduction in Lamtor1 deficient macrophages was not rescued by the supply of exogenous ROS or the induction of endogenous ROS by mitochondrial poisons (Fig 1E and F), though ROS can promote the assembly of NLRP3 inflammasomes (Zhou *et al*, 2011). In addition, DL-all-rac- $\alpha$ -tocopherol suppressed IL-1 $\beta$  release more than D- $\alpha$ -tocopherol even though both have antioxidant properties (Hoppe & Krennrich, 2000). These data suggest there are other mechanisms other than ROS production during the inflammasome activation phase in

**Figure 7. DL-all-rac- $\alpha$ -tocopherol inhibits Lamtor1 and HDAC6 interactions and suppresses inflammasome activation.**

- A Schematic showing the use of a NanoBRET assay to search for inhibitors of Lamtor1–HDAC6 interactions in a library of natural compounds.
- B–F Effects of DL-all-rac- $\alpha$ -tocopherol on the interactions between Lamtor1 and HDAC6. Immunoblot analysis of Lamtor1–Flag co-immunoprecipitated with HDAC6–myc from lysates of HEK293T cells transfected with the indicated plasmids after pretreatments with the DL-all-rac- $\alpha$ -tocopherol (B) or D- $\alpha$ -tocopherol (E) (10  $\mu$ M, overnight). Data are shown as means  $\pm$  SEM. \*\* $P$  < 0.01 by the Student's  $t$ -test,  $n$  = 3 biological replicates. IL-1 $\beta$  secretion upon NLRP3 inflammasome activation after overnight pretreatment with DL-all-rac- $\alpha$ -tocopherol (C) or D- $\alpha$ -tocopherol (F) at the indicated concentrations. ELISA assay showing IL-1 $\beta$  secretion in supernatants from WT THP-1 cells treated with LPS (200 ng/ml, 2 h) and nigericin (15  $\mu$ M, 1 h) after priming with PMA (50 nM, overnight). Data are shown as means  $\pm$  SEM. \* $P$  < 0.05 by one-way ANOVA,  $n$  = 3 biological replicates. (D) IL-6 secretion after overnight pretreatment with DL-all-rac- $\alpha$ -tocopherol. ELISA assay showing IL-6 secretion in supernatants from WT BMDMs treated with LPS (200 ng/ml, overnight) and DL-all-rac- $\alpha$ -tocopherol at the indicated concentrations (overnight). Data are shown as means  $\pm$  SEM. n.s indicates no significant difference by one-way ANOVA,  $n$  = 3 biological replicates.
- G Effects of DL-all-rac- $\alpha$ -tocopherol in an acute gouty arthritis model. MSU crystals (0.5 mg) suspended in 20  $\mu$ l endotoxin-free PBS or PBS control were injected intra-articularly into the tibia-tarsal joint (ankle) of C57BL/6 WT mice with or without DL-all-rac- $\alpha$ -tocopherol. Ankle joint swelling at 24 h was assessed with electronic calipers and with photomicrographs and hematoxylin and eosin-stained sections of ankle joints. Data are shown as means  $\pm$  SEM. \*\* $P$  < 0.01 by the Student's  $t$ -test,  $n$  = 6 mice. Scale bars = 30  $\mu$ m.
- H Effects of DL-all-rac- $\alpha$ -tocopherol in an MSU-induced peritonitis model. Twelve hours after DL-all-rac- $\alpha$ -tocopherol pretreatment, 100  $\mu$ l MSU solution (10 mg/ml) was intraperitoneally injected for 4 h. Peritoneal IL-1 $\beta$  production was then measured by ELISA, and CD11b + Ly6G+ neutrophil recruitment was measured by FACS. Data are shown as means  $\pm$  SEM. \* $P$  < 0.05 by the Student's  $t$ -test,  $n$  = 4 mice (control) and  $n$  = 5 mice (DL-all-rac- $\alpha$ -tocopherol).

Source data are available online for this figure.

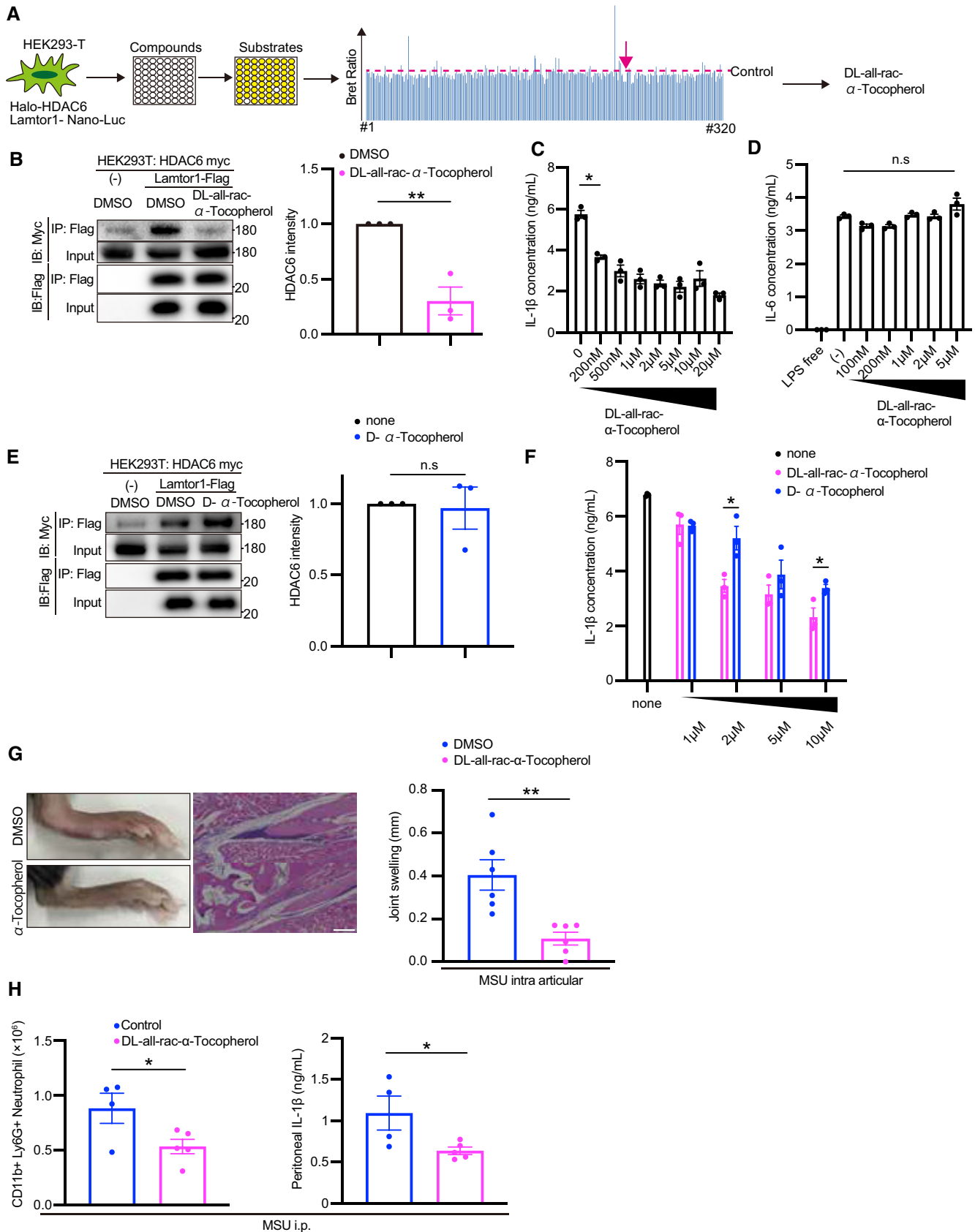
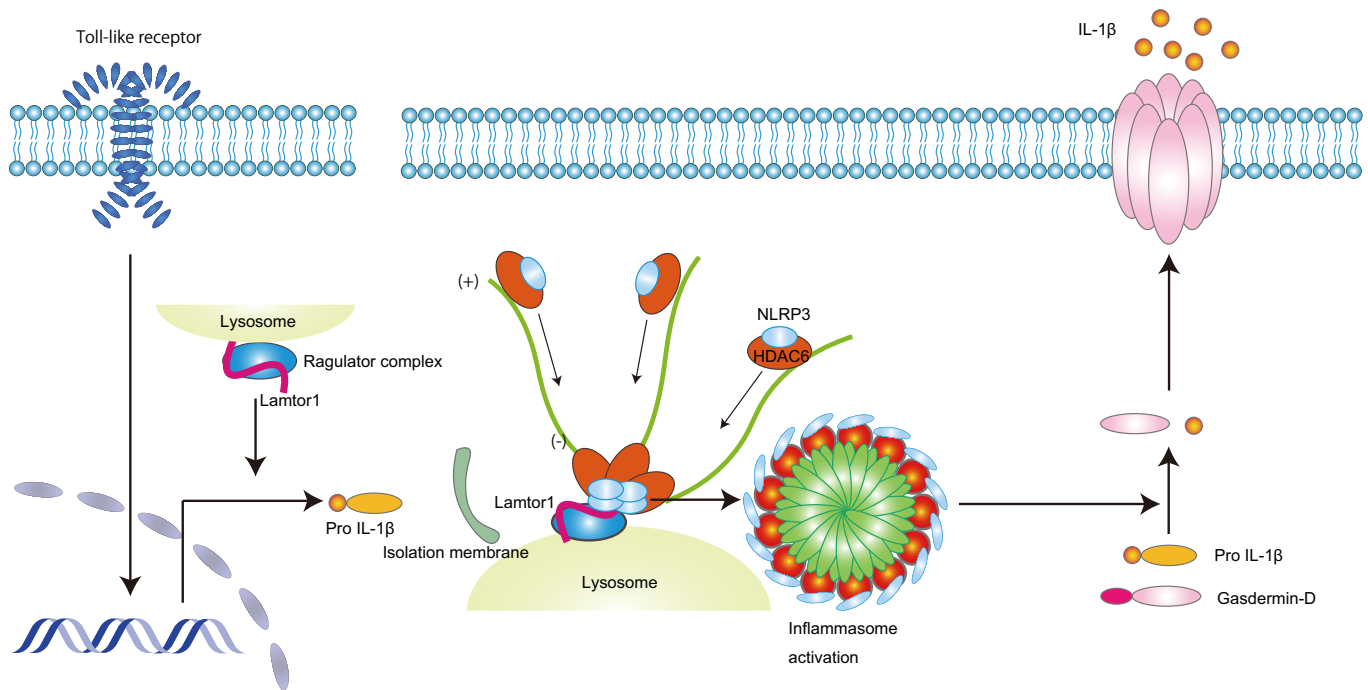


Figure 7.



**Figure 8. The Ragulator complex regulates inflammasome activation through interactions with NLRP3 augmented by HDAC6.**

The Ragulator complex expressed on the lysosomal membrane interacts with HDAC6, which augments the interactions between Lamtor1 and NLRP3, resulting in the activation of the inflammasome.

Lamtor1 KO macrophages. However, it should be noted that we did not address whether ROS could rescue the impaired pyroptosis in Lamtor1-deficient cells. Additionally, the possibility that ROS are not involved in the impairment of NLRP3 inflammasome activation in Lamtor1-deficient cells cannot be completely ruled out, as both sufficient amounts of NLRP3, pro-IL-1 $\beta$ , and gasdermin D and post-transcriptional modifications such as ubiquitination and oxidation are likely required for full inflammasome activation. In addition, the spatiotemporal ROS production and origin of ROS could be important for inflammasome activation and pyroptosis induction. In this context, the relationship between ROS and the Ragulator complex in inflammasome activation and pyroptosis needs to be further elucidated.

In our model, the Ragulator complex mediates inflammasome activation not through the mTOR pathway but rather by protein–protein interactions between the Ragulator complex and HDAC6 and NLRP3. In terms of the relationship between the inflammasome and mTORC1, Moon *et al* (2015) reported that mTORC1-induced HK1-dependent glycolysis regulated NLRP3 inflammasome activity (Moon *et al*, 2015). Evavold *et al* (2021) proposed that mTOR regulates inflammasome-mediated pyroptosis by controlling the production of mitochondrial reactive oxygen species (Evavold *et al*, 2021). In our experiments, we concluded that mTORC1 activity is not necessary for the direct inflammasome activation phase. However, we do not deny the involvement of mTORC1 in other phases of inflammasome activation. In particular, mTOR may contribute to the priming phase of inflammasome activation, since it has a significant effect on transcription. Neither, do we deny the possibility that mTORC1 is indirectly involved in inflammasome activation as

mTORC1 has pleiotropic effects on various cellular homeostasis, so that differences in conditions such as drug concentrations and the cells may easily cause discrepant results.

We demonstrated that the decrease in IL-1 $\beta$  production in Lamtor1-deficient macrophages was independent of TFEB nuclear localization based on the results of the Lamtor1/TFEB double-KO experiments. However, we have to take into account potential compensatory mechanisms involving transcription factor E3 (TFE3), a MiT/TFE family member, because it has redundant roles with TFEB in macrophage activation (Pastore *et al*, 2016) by acting on the same transcription target, and being regulated by the Ragulator complex (Villegas *et al*, 2019).

We have revealed that Lamtor1 interacts with both NLRP3 and HDAC6 and that the absence of HDAC6 attenuates the interaction between Lamtor1 and NLRP3. This raises at least two questions: “What is the role of HDAC6?” and “What is the role of lysosomes?” To address these questions, we have proposed a model in which the lysosome has a dual nature, that is, positively regulating inflammasome activation through interactions with HDAC6 while simultaneously negatively regulating the inflammasome through degradation. Previous studies showed that HDAC6 interacted with NLRP3 (Hwang *et al*, 2015) and promoted the transportation of NLRP3 from the trans-Golgi network to the MTOC via microtubules through an aggresome-like mechanism (Magupalli *et al*, 2020). Considering that the pericentriolar region was enriched in lysosomes (Ren *et al*, 2009), we have suggested that the Ragulator complex on lysosomes may serve as a scaffold that allows NLRP3 transported by HDAC6 to locally increase in density and to form aggresome-like formations. On the other hand, the MTOC, in which HDAC6 transports NLRP3,

acts as a hub to promote the fusion of autophagosomes with lysosomes. It has been shown that autophagy dysfunction can lead to the excessive activation of NLRP3 inflammasomes (Paik *et al*, 2021) and HDAC6 processes aggregates at the MTOC for the autophagic degradation of ubiquitinated pathological aggregates (Kawaguchi *et al*, 2003). In this context, the Ragulator complex may facilitate proximity between NLRP3 and lysosomes by interacting with HDAC6 and function as a built-in checkpoint for inhibiting NLRP3 inflammasome activation, thus allowing for the immediate degradation of the inflammasome.

Our findings indicate a potential therapeutic target for various diseases in which inflammasomes are abnormally activated. Inflammasomes are involved not only in inflammatory diseases such as gout and autoinflammatory syndromes but also in chronic inflammation caused by various metabolic disorders and neurological diseases such as dementia (Swanson *et al*, 2019). Therefore, there is a need to develop therapeutic agents that target inflammasomes. Colchicine, an approved drug for gout and other inflammasome-related diseases, broadly inhibits intracellular function by blocking microtubule polymerization (Deftereos *et al*, 2022). In this study, we have shown that DL-all-rac- $\alpha$ -tocopherol, a synthetic form of vitamin E, may be a potential therapeutic agent that targets inflammasomes by inhibiting the interactions between the Ragulator complex and HDAC6. DL-all-rac- $\alpha$ -tocopherol is already used worldwide for the treatment of hypertension-related symptoms, dyslipidemia, and peripheral circulation disorder with potential antiplatelet effects (Singh *et al*, 2005; Wallert *et al*, 2019). Its efficacy has been thought to be due to its antioxidant effects. However, we suggest another mechanism, namely that DL-all-rac- $\alpha$ -tocopherol inhibits inflammasome activation. Our data showed that D- $\alpha$ -tocopherol did not inhibit the Lamtor1-HDAC6 interaction, and that the DL-all-rac- $\alpha$ -tocopherol reduced IL-1 $\beta$  production more than D- $\alpha$ -tocopherol. These data suggest that the effect of DL-all-rac- $\alpha$ -tocopherol cannot be explained by the antioxidant effect. Although further research is required, for instance, to determine which of the optical isomers of DL-all-rac- $\alpha$ -tocopherol has the highest specificity, this agent can be used to treat chronic NLRP3 inflammasome-related inflammatory diseases.

Collectively, we have provided evidence that the Ragulator complex expressed on the lysosomal membrane plays a critical role in inflammasome activation by interacting with NLRP3, which is augmented by HDAC6. Furthermore, inhibition of the interaction between Lamtor1 and HDAC6 may be an effective therapeutic target for NLRP3 inflammasome-related diseases.

## Materials and Methods

### Mice

*Lamtor1*<sup>flox</sup> mice were generated by Dr. Shigeyuki Nada as described previously (Soma-Nagae *et al*, 2013). *TFEB*<sup>flox</sup> transgenic mice were provided by Dr. Andrea Ballabio (Settembre *et al*, 2012), and *LysM-Cre* transgenic mice were provided by Dr. Shizuo Akira (Takeda *et al*, 1999). Genotyping was performed using primers 5'-AAGGATT CCGAGTTAGAGACTAGGAC-3' and 5'-TGAGGATTCGAGTGGTGAG ATACGA-3' for the *Lamtor1*<sup>flox</sup> and *Lamtor1* alleles, 5'-GTAG AACTGAGTCAAGGCATACTGG-3' and 5'-CAGCCCCCTACCAGCGT

CCC-3' for the *TFEB*<sup>flox</sup> and *TFEB* alleles, and 5'-CTTGCTGTGTGT GTTCTGTGCTGAGG-3' and 5'-GCATAACCAGTGAAACAGCATTG C-3' for the *LysM-Cre-Tg* mice. Myeloid-specific *Lamtor1*<sup>-/-</sup> mice were generated by crossing two strains and backcrossing the progeny to C57BL/6J mice approximately 10 times. Mice were housed under specific pathogen-free conditions with a 12 h light/dark cycle, at a temperature of 22  $\pm$  2°C, and a relative humidity of 50  $\pm$  5%. Mice were fed a standard mouse chow diet, and 3–5 mice were housed in the same cage. The application of animal experiments was approved by the ethical board of the graduate school of medicine, Osaka University (28-008-034). All experiments were performed according to the regulations of Osaka University. Eight- to twelve-week-old mice were used in all experiments. Both male and female mice were used; however, sex was always matched in each experiment. Mice were randomized into control and experimental groups.

### Cells and cell cultures

BMDMs were differentiated as previously described (Kimura *et al*, 2016). In brief, bone marrow cells from the femur and tibia were subjected to red blood cell lysis, and the surviving cells were cultured for 6 days in a differentiation medium. The differentiation medium was comprised of Dulbecco's minimum essential medium (DMEM; Nacalai Tesque, Kyoto, Japan; 50% of total volume), L929 cell culture supernatant (30%), heat-inactivated fetal bovine serum (FBS; Gibco, Thermo Fisher Scientific, Waltham, MA; 20%), and penicillin/streptomycin (1%). THP-1, a human acute monocyte leukemia cell line, was obtained from ATCC (TIB-202), and cultured in RPMI 1640 (Nacalai Tesque) supplemented with 10% FBS, 1% penicillin/streptomycin, and 0.05 mM 2-mercaptoethanol. THP-1 cells were differentiated with 50 nM phorbol 12-myristate 13-acetate (PMA; Sigma-Aldrich, St. Louis, MO) for 1 day. All cells were maintained at 37°C in 5% CO<sub>2</sub>.

### Antibodies, reagents, and fluorescent dyes

Reagents were obtained from the suppliers listed in the Appendix Table S1.

### NanoBRET

Plasmids of HDAC6 tagged with NanoLuc donor at the amino terminus (HDAC6-HTN) and Lamtor1 tagged with NanoLuc acceptor at the carboxy terminus (Lamtor1-NLF-C) were generated using an In-Fusion HD Cloning Kit (Takara Bio, Shiga, Japan) according to the manufacturer's instructions. In brief, cDNA fragments of human Lamtor1, NLRP3, and HDAC6 were ligated to homologous sequences by overlapping PCR using the primers listed in Appendix Table S1, then cloned into the EcoRI-SacI sites of the pNLF1-C [CMV/Hygro] Vector (Accession Number KF811458) for Lamtor1, and the EcoRI-SacI sites of pHTN HaloTag CMV-neo Vector (Accession Number JF920304) for NLRP3 and HDAC6 using the In-Fusion HD Cloning Kit. The transfection of HEK293T cells for the luciferase assays was carried out using Lipofectamine 2000 (Invitrogen, Waltham, MA, USA). Following the addition of Nano-Glo Luciferase Assay Substrate (Promega, Madison, WI, US), luminescence was measured 48 h after transfection using a GloMax Discover Microplate Reader (Promega, Madison, WI, USA).



### Chemical compound library screening

A phytochemical library was obtained from Prestwick Chemical. HEK293T cells transiently expressing HDAC6 HTN and Lamtor1-NLFC, which were treated overnight with chemical compounds diluted to a concentration of 10  $\mu$ M with DMEM. HDAC6-Lamtor1 interactions were examined using the NanoBRET assay, as described above.

### In situ PLA

A Duolink In Situ PLA Kit (Sigma-Aldrich, St. Louis, MO, USA) was used for *in situ* PLAs according to the manufacturer's instructions. At least 10 fields were observed per sample.

### Yeast two-hybrid assay

A yeast two-hybrid assay was performed as previously described (Nakajo et al, 2016). In brief, the PJ69-4A strain was co-transformed with the pACT2 AD and pFBT9 BD plasmids. The transformed cells were grown on an SC-LW (SD/-Lue/-Trp) plate for 3 days at 30°C. Five independent colonies were re-streaked on an SC-LW plate and QDO (SD/-Ade/-His/-Leu/-Trp) followed by incubation for 3 days at 30°C.

### Inflammasome activation

BMDMs ( $1 \times 10^6$  cells/ml) were seeded in 6-well, 24-well, or 96-well plates overnight. Then, after pretreatment with LPS (200 ng/ml) for 4 h, BMDMs were further stimulated with ATP (5 mM) or nigericin (15  $\mu$ M) for 60 min unless otherwise indicated, or with GPN (200 nM) overnight. To investigate AIM2 inflammasome activation, macrophages were primed with LPS (200 ng/ml), then transfected with poly(dA:dT; 5  $\mu$ g/ml) using Lipofectamine 2000 (Invitrogen, Waltham, MA, USA). To investigate pyrin inflammasome activation, macrophages were primed with LPS (200 ng/ml) followed by stimulation with TcdB (0.5  $\mu$ g/ml for 3 h).

### Western blotting

Cells were solubilized in buffer A [1% Nonidet P-40 (NP-40), 50 mM Tris-HCl (pH 7.4), 150 mM NaCl, 1 mM EDTA, 5% glycerol, 2% n-octyl- $\beta$ -D-glucopyranoside] with proteinase inhibitor (Roche, Basel, Switzerland), vortexed for 10 min, and centrifuged at 20,000 g for 15 min at 4°C. Supernatants were mixed with 2  $\times$  Laemmli sample buffer containing 2-mercaptoethanol and denatured for 5 min at 95°C. The reduced samples were electrophoresed in 4–12% Bis-Tris gels (Life Technologies, Carlsbad, CA, USA), transferred to nitrocellulose membranes, and blotted with the antibodies listed in Appendix Table S1. Protein concentrations in SDS-PAGE gel bands were determined using ImageJ software (NIH, Bethesda, MD, USA), and statistical analysis was performed using the Student's *t*-test for two samples and two-way ANOVA for more than two samples.

### Immunoprecipitation

HEK293T cells were transfected with the indicated plasmids using Lipofectamine 3,000 (Invitrogen, Waltham, MA, USA) and

incubated for 24 h. Cells were solubilized with buffer A and centrifuged at 20,000 g for 15 min at 4°C. Immunoprecipitation was performed using the Dynabeads Protein G Immunoprecipitation Kit (10007D, Invitrogen, Waltham, MA, USA). Briefly, after the binding of the antibody to magnetic beads (10 min at room temperature, with rotation), cell lysates and antibody-coated beads were mixed and incubated for 30 min at room temperature. After three washes, proteins were eluted with 2  $\times$  Laemmli sample buffer containing 2-mercaptoethanol and denatured for 5 min at 95°C. The samples were separated by SDS-PAGE and blotted with the indicated antibodies.

### Lyso-IP

Lysosomes were isolated from  $3.0 \times 10^7$  cells treated with 200 ng/ml LPS for 2 h using the Minute Lysosome Isolation Kit (Invent Biotechnologies, Plymouth, MN, USA) according to the manufacturer's instructions. Saturated ammonium sulfate was added to fractionate the eluted protein solution to 25, 50, 75, or 100% of the original volume. Each fraction was purified by methanol-chloroform precipitation and dissolved in a PTS solution, then denatured by heating on a 95°C block incubator for 5 min. Dithiothreitol (Wako, Osaka, Japan) was used for Cys reduction and iodoacetamide (Wako, Osaka, Japan) was used for Cys alkylation. Then, 1% volume of 1  $\mu$ g/ $\mu$ l mass spectrometry-grade trypsin (Trypsin Gold, Promega, Madison, WI, USA) was added and the solution was incubated overnight at 25°C. Trypsinized protein solution was fractionated into eight fractions using an SDB-SCX stage tip (GL Science, Tokyo, Japan). Eight samples from the first fraction of saturated ammonium sulfate were purified with the C18 tip (C-tip, AMR), dried by centrifuge concentrator, and dissolved in a 0.1% aqueous solution of formic acid (FA). The fractionated samples were aligned to an LC-MS system (LC: NanoElute, MS: tims TOF Pro, Bruker, Billerica, MA, USA); LC-mobile phase A: 0.1% FA in water; B: 0.1% FA in acetonitrile; separation column: Nikkyo C18 column NTCC-360 (75  $\mu$ m  $\times$  150 mm, 3- $\mu$ m particle). The LC separation gradient was set from 2% B to 35% B in 60 min at a 400 nl/min flow rate. The acquired mass spectrometry data were analyzed using a MASCOT server (ver. 2.7, Matrix Science) with the SwissProt database, and the data from the eight fractions were combined using Scaffold software (Proteome Software, Portland, OR, USA).

### Pharmacological inhibition

BMDMs were primed with 200 ng/ml LPS with or without the HDAC6 inhibitor rocilinostat (30 mM; Selleckchem, Houston, TX, USA) or tubacin (5–40 mM; Enzo Life Sciences, New York, NY, USA). Four hours after the drug treatment, inflammasome activation was performed with ATP for 60 min. To examine the effect of the mTOR inhibitors, BMDMs were primed with LPS before or after the Rapamycin or Torin-1 treatment at the indicated concentration for 4 h. Afterward, inflammasome activation was performed with nigericin for 60 min. To examine the effects of the DL-all-rac- $\alpha$ -tocopherol, BMDMs were pretreated overnight with DL-all-rac- $\alpha$ -tocopherol at the indicated concentrations, then stimulated with LPS. The inflammasome activators were added as described above.

## Expression vector cloning

The generation of cDNA encoding *Lamtor1* (Met1-Pro161) fused C-terminally to the 3 × FLAG tag of *Lamtor1* was previously described (Nakatani *et al*, 2021). A mutant fragment of *Lamtor1* in which G2 was replaced with alanine (G2A) was ligated to the 3 × FLAG sequence by overlapping PCR using the primers listed in the Appendix Table S1. Each cDNA fragment was then cloned into the *NotI*–*Bam*HI sites of the CSII-EF-IRES2-Venus vector provided by Dr. Hiroyuki Miyoshi (Keio University) using the In-Fusion HD Cloning Kit (Takara, Shiga, Japan). cDNA encoding the full-length or truncated form of *Lamtor1* was fused C-terminally to the 3 × V5 tag and a truncated cDNA fragment of human *Lamtor1* ( $\Delta$ T145–161, Met1-Ser144, deletion of C-terminal tail;  $\Delta$ 95–161, Met1-Val94, deletion of loop,  $\alpha$ 3,  $\alpha$ 4 helix, and C-terminal tail) was fused C-terminally to the 3 × FLAG sequence, which was synthesized by Eurofin Genomics (Tokyo, Japan) and cloned into the *NotI*–*Bam*HI sites of vector CSII-EF-IRES2-Venus using the In-Fusion HD Cloning Kit. To generate cDNA encoding full-length *Lamtor1* fused C-terminally to tdTomato, *Lamtor1* was cloned into tdTomato-N1 vectors, then cloned into the *NotI*–*Bam*HI sites of CSII-EF-IRES2-Venus vector using the In-Fusion HD Cloning Kit. cDNA encoding full-length NLRP3 was fused at the C-terminus to a 3 × FLAG tag and cloned into the lentiviral vector CSII-EF-IRES2-Venus. cDNA encoding full-length ASC was fused at the C-terminus to GFP and cloned into the *EcoRI*–*KpnI* sites of pEGFP-N1. For the generation of cDNA encoding HDAC6 (Met1-Gly1286) fused C-terminally to the 3 × Myc tag, pcDNA3.1-HDAC6-FLAG (Addgene plasmid #30482), which was subcloned into the *NotI*–*HpaI* sites of vector CSII-EF-IRES2-Venus using the In-Fusion HD Cloning Kit. cDNA encoding Caspase-1 p10 and p20 was ligated to the 3 × FLAG sequence by overlapping PCR and cloned into the *NotI*–*Bam*HI sites of the CSII-EF-IRES2-Venus vector using the In-Fusion HD Cloning Kit. A vector carrying the active form of GSDMD (NT-GSDMD) was synthesized by VectorBuilder Japan (Yokohama, Japan). pcDNA-HDAC6-FLAG was a gift from Tso-Pang Yao (Kawaguchi *et al*, 2003) and tdTomato-N1 was a gift from Michael Davidson, Nathan Shaner, and Roger Tsien (Shaner *et al*, 2004). Transfectants were selected and single clones were screened by western blotting. For the yeast two-hybrid assay, the cDNAs of HDAC6, *Lamtor1*, *Lamtor2*, and NLRP3 were ligated into pACT2 or pFBT9 vectors.

## Generation of knockout or knockdown cell lines

*Lamtor1*-deficient THP-1 cells were generated as previously described (Nakatani *et al*, 2021). HDAC6 knockdowns were performed using lentiviral plasmids expressing shRNAs specific for human HDAC6, and the target sequence was CCGTAATGGAACCT-CAGCACAT (TRCN0000004842, Sigma-Aldrich).

## CRISPR-Cas9 generation of THP-1 knock-in cell lines carrying flag tag sequences for the *Lamtor1* gene

To generate THP-1 knock-in cell lines carrying Flag tag to the C-terminus of *Lamtor1*, cells stably expressing Cas9 were co-transfected with a mixture of several sgRNAs and donor double-stranded (ds) DNA using Avalanche-Omni transfection reagent (EZ Biosystems). Target sequences used for the knock-in of Flag tag

were 5'-CCTGAGACAGAGAGGGGCCGGGG-3', 5'-GACCTGAGACAGAGAGGGGCCGG-3', and 5'-CCTGGAGACCTGAGACAGAGAGG-3'. The dsDNA donor template used to insert the Flag tag sequence into the *Lamtor1* gene was designed with 500-bp homologous arms flanking the CRISPR-Cas9 cleavage site, and each protospacer adjacent motif sequence was mutated to avoid targeting by the sgRNA/Cas9 complex. After the isolation of the monoclonal cell populations, knock-in of Flag tag was confirmed by western blotting.

## Enzyme-linked immunosorbent assay

Serum cytokine levels were measured using the DuoSet ELISA Development System (R&D Systems).

## Immunostaining and fluorescence microscopy

For immunostaining, cells were fixed with 4% paraformaldehyde and permeabilized with 0.1% Triton X-100 in PBS, before incubation with primary antibodies followed by Alexa Fluor secondary antibodies. Nuclei were stained with DAPI in a mounting medium (ProLong Gold with DAPI, Thermo). For imaging with multiple channels, extensive control experiments were performed to ensure that there was no nonspecific staining or crosstalk between channels. These control experiments included: (i) using cells that lacked one of the proteins of interest, and (ii) performing staining without one of the primary or secondary antibodies. Fluorescence images of fixed cells were obtained with an FV3000 confocal laser scanning microscope (Olympus, Tokyo, Japan).

## Crystal-induced ankle arthritis model

C57BL/6 WT mice were subcutaneously anesthetized with ketamine and xylazine, and MSU crystals (0.5 mg) suspended in 20  $\mu$ l endotoxin-free PBS or the PBS control was injected intra-articularly into the right and left tibia-tarsal joints, respectively. DL-all-rac- $\alpha$ -tocopherol (100 mM, 10  $\mu$ l) was injected into the left tibia-tarsal joint once with MSU crystals. After 24 h, joint sizes were measured by blinded electronic caliper and mice were euthanized to collect joints for hematoxylin and eosin staining.

## Mouse peritonitis model

C57BL/6 WT or myeloid-specific *Lamtor1* KO mice were intraperitoneally injected with LPS (10 mg/kg) or 600  $\mu$ l alum solution (20 mg/ml) for 6 h, or with 100  $\mu$ l MSU solution (10 mg/ml) for 4 h. The IL-1 $\beta$  content in serum (LPS) and lavage fluid (alum) was measured by ELISA. To assess the effect of DL-all-rac- $\alpha$ -tocopherol, 4 mg was injected intraperitoneally with 1 mg MSU crystals. For the screening of immune cell populations, peritoneal infiltrating cells were stained with the indicated antibodies and analyzed on a FACS Canto II (BD Biosciences).

## Statistical analysis

All statistical analyses were conducted using GraphPad Prism version 8. Normally distributed data were compared using the Student's *t*-test or one-way ANOVA plus *post hoc* analysis, and are presented as the means  $\pm$  SEM. A value of *P* < 0.05 was considered significant.

## Data availability

All data derived from the quantitative proteomics analysis of the isolated lysosomes has been deposited in the publicly available Proteomics Identification database under the accession code PXD0033497 (<https://www.ebi.ac.uk/pride/archive/projects/PXD0033497>).

**Expanded View** for this article is available [online](#).

## Acknowledgements

I would like to take this opportunity to thank T.Y. for years of collaboration and advice. This study was supported in part by a Core Research for Evolutionary Science and Technology (CREST) grant from the Japan Science and Technology Agency (JST; JPMJCR16G2 to H.T.); the Center of Innovation Program (COI-STREAM) of the Ministry of Education, Culture, Sports, Science and Technology of Japan (MEXT; to A.K.); the Japan Agency for Medical Research and Development (AMED)—CREST (15652237 to A.K.); the Japan Society for the Promotion of Science (JSPS) KAKENHI (JP18H05282 to A.K.); and the Japan Agency for Medical Research and Development (AMED; JP18cm016335, JP18cm059042 and 223fa627002h0001 to A.K.), Research Grant from Japan Agency for Medical Research and Development—Core Research for Evolutional Science and Technology (AMED—CREST; 22gm1810003h0001 to A.K.). This work was also supported by the Italian Telethon Foundation (TIGEM institutional grant), European Research Council H2020 AdG (LYSOSOMICS 694282 to A.B.), and Associazione Italiana per la Ricerca sul Cancro A.I.R.C. (IG-22103 to A.B.).

## Author contributions

**Kohei Tsujimoto:** Conceptualization; data curation; formal analysis; funding acquisition; validation; investigation; methodology; writing – original draft; project administration; writing – review and editing. **Tatsunori Jo:** Investigation; methodology. **Daiki Nagira:** Investigation; methodology. **Hachiro Konaka:** Resources; methodology. **Jeong Hoon Park:** Investigation; methodology. **Shin-ichiro Yoshimura:** Investigation; methodology; writing – review and editing. **Akinori Ninomiya:** Resources; investigation; methodology. **Fuminori Sugihara:** Resources; investigation; methodology. **Takehiro Hirayama:** Methodology. **Eri Itotagawa:** Methodology. **Yusei Matsuzaki:** Methodology. **Yuki Takaichi:** Methodology. **Wataru Aoki:** Methodology; writing – review and editing. **Shotaro Saita:** Methodology; writing – review and editing. **Shuheji Nakamura:** Methodology; writing – review and editing. **Andrea Ballabio:** Methodology; writing – review and editing. **Shigeyuki Nada:** Methodology; writing – review and editing. **Masato Okada:** Methodology; writing – review and editing. **Hyota Takamatsu:** Conceptualization; supervision; funding acquisition; investigation; methodology; writing – original draft; project administration; writing – review and editing. **Atsushi Kumanogoh:** Supervision; funding acquisition; methodology; writing – review and editing.

## Disclosure and competing interests statement

The authors except A.B. have no conflicting financial interests. A.B. is a cofounder of CASMA Therapeutics and an Advisory board member of Next Generation Diagnostics, Avilar Therapeutics, and Coave Therapeutics.

## References

de Araujo MEG, Naschberger A, Furnrohr BG, Stasyk T, Dunzendorfer-Matt T, Lechner S, Welti S, Kremser L, Shivalingaiah G, Offterdinger M et al (2017)

- Crystal structure of the human lysosomal mTORC1 scaffold complex and its impact on signaling. *Science* 358: 377–381
- Ballabio A, Bonifacino JS (2020) Lysosomes as dynamic regulators of cell and organismal homeostasis. *Nat Rev Mol Cell Biol* 21: 101–118
- Burton GW, Traber MG (1990) Vitamin E: antioxidant activity, biokinetics, and bioavailability. *Annu Rev Nutr* 10: 357–382
- Chen J, Chen ZJ (2018) PtdIns4P on dispersed trans-Golgi network mediates NLRP3 inflammasome activation. *Nature* 564: 71–76
- Colville A, Liu J-Y, Thomas S, Ishak HD, Zhou R, Klein JDD, Morgens DW, Goshayeshi A, Salvi JS, Yao D et al (2022) Death-seq identifies regulators of cell death and senolytic therapies. *bioRxiv* <https://doi.org/10.1101/2022.04.01.486768> [PREPRINT]
- Condon KJ, Orozco JM, Adelman CH, Spinelli JB, van der Helm PW, Roberts JM, Kunchok T, Sabatini DM (2021) Genome-wide CRISPR screens reveal multitiered mechanisms through which mTORC1 senses mitochondrial dysfunction. *Proc Natl Acad Sci USA* 118: e2022120118
- Deftereos SG, Beerkens FJ, Shah B, Giannopoulos G, Vrachatis DA, Giotaki SG, Siasos G, Nicolas J, Arnott C, Patel S et al (2022) Colchicine in cardiovascular disease: in-depth review. *Circulation* 145: 61–78
- Devant P, Boršič E, Ngwa EM, Thiagarajah JR, Hafner-Bratkovič I, Evavold CL, Kagan JC (2022) The pore-forming protein gasdermin D is a cellular redox sensor. *bioRxiv* <https://doi.org/10.1101/2022.03.11.484021> [PREPRINT]
- Elliott EI, Sutterwala FS (2015) Initiation and perpetuation of NLRP3 inflammasome activation and assembly. *Immunity* 42: 35–52
- Evavold CL, Kagan JC (2019) Inflammasomes: threat-assessment organelles of the innate immune system. *Immunity* 51: 609–624
- Evavold CL, Hafner-Bratkovič I, Devant P, D'Andrea JM, Ngwa EM, Boršič E, Doench JG, LaFleur MW, Sharpe AH, Thiagarajah JR et al (2021) Control of gasdermin D oligomerization and pyroptosis by the regulator-rag-mTORC1 pathway. *Cell* 184: 4495–4511.e19
- Franchi L, Eigenbrod T, Munoz-Planillo R, Nunez G (2009) The inflammasome: a caspase-1-activation platform that regulates immune responses and disease pathogenesis. *Nat Immunol* 10: 241–247
- Grozinger CM, Hassig CA, Schreiber SL (1999) Three proteins define a class of human histone deacetylases related to yeast Hda1p. *Proc Natl Acad Sci USA* 96: 4868–4873
- Guarda G, Braun M, Staehli F, Tardivel A, Mattmann C, Förster I, Farlik M, Decker T, Du Pasquier RA, Romero P et al (2011) Type I interferon inhibits interleukin-1 production and inflammasome activation. *Immunity* 34: 213–223
- Hayama Y, Kimura T, Takeda Y, Nada S, Koyama S, Takamatsu H, Kang S, Ito D, Maeda Y, Nishide M et al (2018) Lysosomal protein Lamtor1 controls innate immune responses via nuclear translocation of transcription factor EB. *J Immunol* 200: 3790–3800
- Hein MY, Weissman JS (2022) Functional single-cell genomics of human cytomegalovirus infection. *Nat Biotechnol* 40: 391–401
- Hoppe PP, Krennrich G (2000) Bioavailability and potency of natural-source and all-racemic alpha-tocopherol in the human: a dispute. *Eur J Nutr* 39: 183–193
- Hwang I, Lee E, Jeon SA, Yu JW (2015) Histone deacetylase 6 negatively regulates NLRP3 inflammasome activation. *Biochem Biophys Res Commun* 467: 973–978
- Jia J, Abudu YP, Claude-Taupin A, Gu Y, Kumar S, Choi SW, Peters R, Mudd MH, Allers L, Salemi M et al (2018) Galectins control mTOR in response to endomembrane damage. *Mol Cell* 70: 120–135.e28
- Kawaguchi Y, Kovacs JJ, McLaurin A, Vance JM, Ito A, Yao TP (2003) The deacetylase HDAC6 regulates aggresome formation and cell viability in response to misfolded protein stress. *Cell* 115: 727–738

- Kim E, Goraksha-Hicks P, Li L, Neufeld TP, Guan KL (2008) Regulation of TORC1 by rag GTPases in nutrient response. *Nat Cell Biol* 10: 935–945
- Kimura T, Nada S, Takegahara N, Okuno T, Nojima S, Kang S, Ito D, Morimoto K, Hosokawa T, Hayama Y et al (2016) Polarization of M2 macrophages requires Lamtor1 that integrates cytokine and amino-acid signals. *Nat Commun* 7: 13130
- Liu GY, Sabatini DM (2020) mTOR at the nexus of nutrition, growth, ageing and disease. *Nat Rev Mol Cell Biol* 21: 183–203
- Magupalli VG, Negro R, Tian Y, Hauenstein AV, Di Caprio G, Skillern W, Deng Q, Orning P, Alam HB, Maliga Z et al (2020) HDAC6 mediates an aggresome-like mechanism for NLRP3 and pyrin inflammasome activation. *Science* 369: eaas8995
- Moon JS, Hisata S, Park MA, DeNicola GM, Ryter SW, Nakahira K, Choi AMK (2015) mTORC1-induced HK1-dependent glycolysis regulates NLRP3 inflammasome activation. *Cell Rep* 12: 102–115
- Nada S, Hondo A, Kasai A, Koike M, Saito K, Uchiyama Y, Okada M (2009) The novel lipid raft adaptor p18 controls endosome dynamics by anchoring the MEK-ERK pathway to late endosomes. *EMBO J* 28: 477–489
- Nakajo A, Yoshimura S, Togawa H, Kunii M, Iwano T, Izumi A, Noguchi Y, Watanabe A, Goto A, Sato T et al (2016) EHBP1L1 coordinates Rab8 and Bin1 to regulate apical-directed transport in polarized epithelial cells. *J Cell Biol* 212: 297–306
- Nakatani T, Tsujimoto K, Park J, Jo T, Kimura T, Hayama Y, Konaka H, Morita T, Kato Y, Nishide M et al (2021) The lysosomal Ragulator complex plays an essential role in leukocyte trafficking by activating myosin II. *Nat Commun* 12: 3333
- Paik S, Kim JK, Silwal P, Sasakawa C, Jo EK (2021) An update on the regulatory mechanisms of NLRP3 inflammasome activation. *Cell Mol Immunol* 18: 1141–1160
- Pastore N, Brady OA, Diab HI, Martina JA, Sun L, Huynh T, Lim JA, Zare H, Raben N, Ballabio A et al (2016) TFEB and TFE3 cooperate in the regulation of the innate immune response in activated macrophages. *Autophagy* 12: 1240–1258
- Perera RM, Zoncu R (2016) The lysosome as a regulatory hub. *Annu Rev Cell Dev Biol* 32: 223–253
- Ranard KM, Erdman JW (2018) Effects of dietary RRR  $\alpha$ -tocopherol vs all-racemic  $\alpha$ -tocopherol on health outcomes. *Nutr Rev* 76: 141–153
- Ren PH, Lauckner JE, Kachirskaja I, Heuser JE, Melki R, Kopito RR (2009) Cytoplasmic penetration and persistent infection of mammalian cells by polyglutamine aggregates. *Nat Cell Biol* 11: 219–225
- Sancak Y, Bar-Peled L, Zoncu R, Markhard AL, Nada S, Sabatini DM (2010) Ragulator-rag complex targets mTORC1 to the lysosomal surface and is necessary for its activation by amino acids. *Cell* 141: 290–303
- Sardiello M, Palmieri M, di Ronza A, Medina DL, Valenza M, Gennarino VA, Di Malta C, Donaudo F, Embrione V, Polishchuk RS et al (2009) A gene network regulating lysosomal biogenesis and function. *Science* 325: 473–477
- Saxton RA, Sabatini DM (2017) mTOR signaling in growth, metabolism, and disease. *Cell* 169: 361–371
- Sborgi L, Rühl S, Mulvihill E, Pipercevic J, Heilig R, Stahlberg H, Farady CJ, Müller DJ, Broz P, Hiller S (2016) GSDMD membrane pore formation constitutes the mechanism of pyroptotic cell death. *EMBO J* 35: 1766–1778
- Settembre C, Zoncu R, Medina DL, Vetrini F, Erdin S, Huynh T, Ferron M, Karsenty G, Vellard MC, Facchinetti V et al (2012) A lysosome-to-nucleus signalling mechanism senses and regulates the lysosome via mTOR and TFEB. *EMBO J* 31: 1095–1108
- Shaner NC, Campbell RE, Steinbach PA, Giepmans BN, Palmer AE, Tsien RY (2004) Improved monomeric red, orange and yellow fluorescent proteins derived from *Drosophila* sp. red fluorescent protein. *Nat Biotechnol* 22: 1567–1572
- Shi J, Zhao Y, Wang K, Shi X, Wang Y, Huang H, Zhuang Y, Cai T, Wang F, Shao F (2015) Cleavage of GSDMD by inflammatory caspases determines pyroptotic cell death. *Nature* 526: 660–665
- Singh U, Devaraj S, Jialal I (2005) Vitamin E, oxidative stress, and inflammation. *Annu Rev Nutr* 25: 151–174
- Soma-Nagae T, Nada S, Kitagawa M, Takahashi Y, Mori S, Oneyama C, Okada M (2013) The lysosomal signaling anchor p18/LAMTOR1 controls epidermal development by regulating lysosome-mediated catabolic processes. *J Cell Sci* 126: 3575–3584
- Sorbara MT, Girardin SE (2011) Mitochondrial ROS fuel the inflammasome. *Cell Res* 21: 558–560
- Swanson KV, Deng M, Ting JP (2019) The NLRP3 inflammasome: molecular activation and regulation to therapeutics. *Nat Rev Immunol* 19: 477–489
- Takeda K, Clausen BE, Kaisho T, Tsujimura T, Terada N, Förster I, Akira S (1999) Enhanced Th1 activity and development of chronic enterocolitis in mice devoid of Stat3 in macrophages and neutrophils. *Immunity* 10: 39–49
- Torres R, Macdonald L, Croll SD, Reinhardt J, Dore A, Stevens S, Hylton DM, Rudge JS, Liu-Bryan R, Terkeltaub RA et al (2009) Hyperalgesia, synovitis and multiple biomarkers of inflammation are suppressed by interleukin 1 inhibition in a novel animal model of gouty arthritis. *Ann Rheum Dis* 68: 1602–1608
- Verdel A, Khochbin S (1999) Identification of a new family of higher eukaryotic histone deacetylases. Coordinate expression of differentiation-dependent chromatin modifiers. *J Biol Chem* 274: 2440–2445
- Villegas F, Lehalle D, Mayer D, Rittirsch M, Stadler MB, Zinner M, Olivieri D, Vabres P, Duplomb-Jego L, De Bont ESJM et al (2019) Lysosomal signaling licenses embryonic stem cell differentiation via inactivation of Tfe3. *Cell Stem Cell* 24: 257–270.e58
- Wallert M, Ziegler M, Wang X, Maluenda A, Xu X, Yap ML, Witt R, Giles C, Kluge S, Hortmann M et al (2019)  $\alpha$ -Tocopherol preserves cardiac function by reducing oxidative stress and inflammation in ischemia/reperfusion injury. *Redox Biol* 26: 101292
- Yonehara R, Nada S, Nakai T, Nakai M, Kitamura A, Ogawa A, Nakatsumi H, Nakayama KI, Li S, Standley DM et al (2017) Structural basis for the assembly of the Ragulator-rag GTPase complex. *Nat Commun* 8: 1625
- Zheng ZZ, Deng WY, Bai Y, Miao R, Mei SL, Zhang ZB, Pan YD, Wang Y, Min R, Deng F et al (2021) The lysosomal rag-Ragulator complex licenses RIPK1-and caspase-8-mediated pyroptosis by Yersinia. *Science* 372: eabg0269
- Zhou R, Yazdi AS, Menu P, Tschopp J (2011) A role for mitochondria in NLRP3 inflammasome activation. *Nature* 469: 22–225